MARIA S. MERIAN-Berichte 10-3

Geosphere-biosphere studies at the Logatchev hydrothermal field, Mid-Atlantic Ridge at 15°N

HYDROMAR VII

Cruise No. 10, Leg 3

11.01. – 13.02.2009, Las Palmas (Spain) – Fort de France (France)

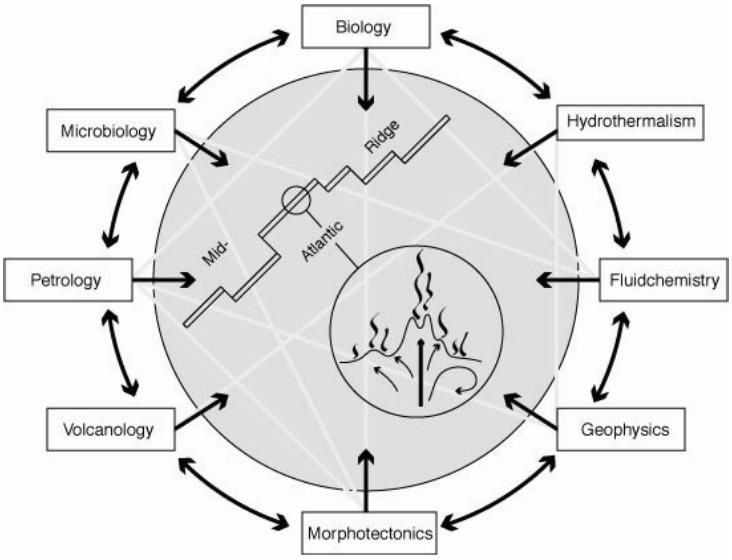

N. Dubilier, F. Abegg, C. Borowski, D. Fink, P. Franke, D. Garbe-Schönberg, P. Hach, A. Heddaeus, C. Hinz, S. Hourdez, C. I Huang, H. Huusmann, F.R. Karbe, V. Klevenz, E. Labahn, M. Perner, M. Peters, M. Pieper, W. Queisser, N. Rychlik, I. Suck, M. Warmuth

Editorial Assistance:

Senatskommission für Ozeanographie der Deutschen Forschungsgemeinschaft
MARUM – Zentrum für Marine Umweltwissenschaften der Universität Bremen

Leitstelle Deutsche Forschungsschiffe
Institut für Meereskunde der Universität Hamburg

2011

Table of Content

1 Summary

RV MARIA S. MERIAN cruise MSM 10-3 was the last in a series of cruises to the Logatchev hydrothermal vent field at 15°N on the Mid-Atlantic Ridge (MAR) as part of the German Research Foundation's Priority Program SPP 1144 "From the Mantle to the Ocean". The goal of SPP1144 was to better understand the geology, chemistry, and biology of hydrothermal vents on the slow-spreading MAR. This cruise had three main goals: 1) to continue and conclude time series studies on the spatial and temporal variability of vent fluids and their effect on vent biota, 2) to better understand how plumes that rise from the Logatchev vents are dispersed in the water column, and how currents and tides influence this dispersal, and 3) to determine the fine structure of the Logatchev hydrothermal vent field and adjoining areas using high-resolution bathymetric mapping. Participating institutions were the Max Planck Institute for Marine Microbiology, the IFM-Geomar, the University of Kiel, the University of Hamburg, the Jacob's University Bremen, and the French CNRS (Biological Station of Roscoff). The main working tools were the ROV (Remotely Operated Vehicle) Kiel 6000 for Goal 1, a CTD-Rosette, Miniature Autonomous Plume Recorders (MAPRs), and oceanographic moorings for Goal 2, and the ship's Kongsberg EM120 multibeam echosounder for Goal 3. Although weather conditions allowed only five ROV dives in the Logatchev working area, we addressed all goals successfully and recovered all scientific instruments that had been deployed during earlier cruises.

Zusammenfassung

FS MARIA-S.-MERIAN-Reise MSM 10/3 war die letzte in einer Reihe von Fahrten zum Logatchev Hydrothermalfeld bei 15°N auf dem Mittelatlantischen Rücken (MAR) im Rahmen des DFG Schwerpunktprogramms SPP 1144 „Vom Mantel Zum Ozean". Übergeordenetes Ziel des SPP 1144 war es ein besseres Verständnis der Geologie, des Chemismus und der Biologie von Hydrothermalquellen am langsam spreizenden MAR zu erlangen. Für MSM 10/3 standen drei Ziele im Vordergrund: 1) Fortführung und Abschluss der mit den vorherigen Fahrten begonnenen Zeitserienuntersuchungen, 2) ein besseres Verständnis darüber erlangen, wie sich die vom Logatchev Hydrothermalfeld aufsteigenden hydrothermalen Plumes ausbreiten und durch tidale Strömungen beeinflusst werden und 3) Bestimmung der geomorphologischen Feinstruktur um das Logatchev Hydrothermalfeld und angrenzenden Regionen mithilfe hochauflösender bathymetrischer Kartierung. Teilnehmende Institute waren das Max-Planck-Institut für Marine Mikrobiologie Bremen, das IFM-Geomar, Kiel, die Universität Kiel, die Universit Hamburg, die Jacobs-Universität Bremen und das französische CNRS (Biologische Station Roscoff). Hauptarbeitsgeräte waren das ROV (Remotely Operated Vehicle) Kiel 6000 (Ziel 1), CTD/Rosette, Miniature Autonomous Plume Recorders (MAPRs), und eine ozeanographische Auslegung (Ziel 2), sowie das schiffseigene Kongsberg EM120 Fächerecholt (Ziel 3). Obwohl anhaltend starke Ostwinde nur fünf ROV-Tauchgänge im Logatchev-Arbeitsgebiet zuließen, wurden alle Ziel erfolgreich verfolgt und alle wissenschaftlichen Messinstrumente geborgen, die von vorangehenden Fahrten ausgebracht wurden.

2 Participants

Name	Discipline	Institution
Dubilier, Nicole, Dr.	Symbioses / Chief Scientist	MPI-Bremen
Klevenz, Verena	Fluid geochemistry, trace elements	JU-Bremen
Hach, Philipp	Fluid geochemistry, trace elements	JU-Bremen
Garbe-Schönberg, Dieter, Dr.	Fluid geochemistry, trace elements	Uni Kiel
Peters, Marc	Fluid geochemistry, sulfur species	Uni Münster
Warmuth, Marco	Fluid geochemistry, dissolved gases	Uni HH IfBM
Heddaeus, Annette	Fluid geochemistry, dissolved gases	Uni HH IfBM
Perner, Mirjam, Dr.	Microbiology	Uni HH BKF
Rychlik, Nicolas	Microbiology	Uni HH BKF
Huang; Chia-I	Microbiology	MPI-Bremen
Borowski, Christian, Dr.	Symbioses	MPI-Bremen
Fink, Dennis	Symbioses	MPI-Bremen
Hourdez, Stéphane, Dr.	Mass Spectrometer	Roscoff
Karbe, Fritz	Oceanography	IFM-Geomar
Abegg, Fritz	ROV team	IFM-Geomar
Pieper, Martin	ROV team	IFM-Geomar
Hinz, Claus	ROV team	IFM-Geomar
Huusmann, Hannes	ROV team	IFM-Geomar
Suck, Inken	ROV team	IFM-Geomar
Labahn, Erik	ROV team	IFM-Geomar
Queisser, Wolfgang	ROV team	IFM-Geomar
Franke, Phillip	ROV team	Marum
Müller, Reinhard, Dr.	Ship's doctor	Briese

MPI-Bremen	Max Planck Institute for Marine Microbiology, Celsiusstr. 1, 28359 Bremen
JU-Bremen	Jacobs University Bremen, PO box 750561 28725 Bremen
Uni HH IfBM	University of Hamburg Hamburg, Institute for Biogeochemistry and Marine Chemistry, Bundesstr. 55, 20146 Hamburg
Uni HH BKF	University of Hamburg, Department of Biology, Biocenter Klein Flottbek, Microbiology and Biotechnology
Uni Kiel	Institute for Geosciences, Christian-Albrechts Universität Kiel, Olshausenstr. 40, 24118 Kiel
Uni Münster	Westfälische Wilhelms-Universität Münster, Geologisch-Paläontologisches Institut
IFM-Geomar	Leibniz Institute of Marine Sciences, Wischhofstr 1-3, 24148 Kiel
Roscoff	Biological Station Roscoff, CNRS-Universitée Pierre et Marie Curie, UMR 7144, Equipe Ecophysiologie: Adaptation et Evolution Moléculaires 29680 Roscoff, France
Marum	Marum Center for Marine Environmental Sciences, Leobenerstr. 28359 Bremen
Briese	Briese Schiffahrts GmbH & Co. KG, Research Vessel Department

3. Research Program

(N. Dubilier)

RV MARIA S. MERIAN cruise MSM 10-3 was the last in a series of nearly yearly cruises since 2004 to the Logatchev hydrothermal vent field at 15°N on the Mid-Atlantic Ridge (MAR). These cruises were part of the German Research Foundation's Priority Program SPP 1144 "From the Mantle to the Ocean" with the goal of gaining a better understanding of the geology, chemistry, and biology of hydrothermal vents on the slow-spreading MAR. Scientists from the Max Planck Institute for Marine Microbiology, the IFM-Geomar, the University of Kiel, the University of Hamburg, the Jacob's University Bremen, and the French CNRS (Biological Station of Roscoff) participated in this cruise.

The cruise, called Hydromar VII, was centered around three goals: 1) to continue and conclude time series studies on the spatial and temporal variability of vent fluids and their effect on vent biota, 2) to better understand how plumes that rise from the Logatchev vents are dispersed in the water column, and how currents and tides influence this dispersal, and 3) to determine the fine structure of the Logatchev hydrothermal vent field and adjoining areas using high-resolution bathymetric mapping. Our main working tools were the ROV (Remotely Operated Vehicle) Kiel 6000 for Goal 1, a CTD-Rosette, Miniature Autonomous Plume Recorders (MAPRs), and oceanographic moorings for Goal 2, and the ship's Kongsberg EM120 multibeam echosounder for Goal 3.

These investigations contributed to answering the following core interdisciplinary questions of the SPP 1144: 1) What factors govern where tectonic, magmatic, hydrothermal, and biological processes occur on spreading axes? 2) How do biological and hydrothermal processes interact? 3) What are the time scales at which processes at spreading axes occur?

4. Narrative of the Cruise

(N. Dubilier)

The RV MARIA S. MERIAN left Las Palmas on January 11th, three days later than originally planned, because problems with customs delayed the loading of the ROV and scientific containers onto the ship. On the second day of transit to our working area, the Logatchev hydrothermal vent field at 14°45' N, 44°58' W on the Mid-Atlantic Ridge (MAR), we used the ship's multibeam echosounder for bathymetric mapping of a seamount at 25°47' N, 26°15' W. A ROV test dive at the seamount down to 1800 m water depth was successful and revealed lava-like black structures and typical seamount fauna. The total transit time of six days to Logatchev was used for safety instructions and a safety drill, and for setting up the labs and preparing instruments and equipment, including the ROV, for station work. In the evenings, the scientists gave talks about their research and the work planned for the cruise, including a more general talk for the ship's crew, while the ROV team gave an introduction to the Kiel 6000.

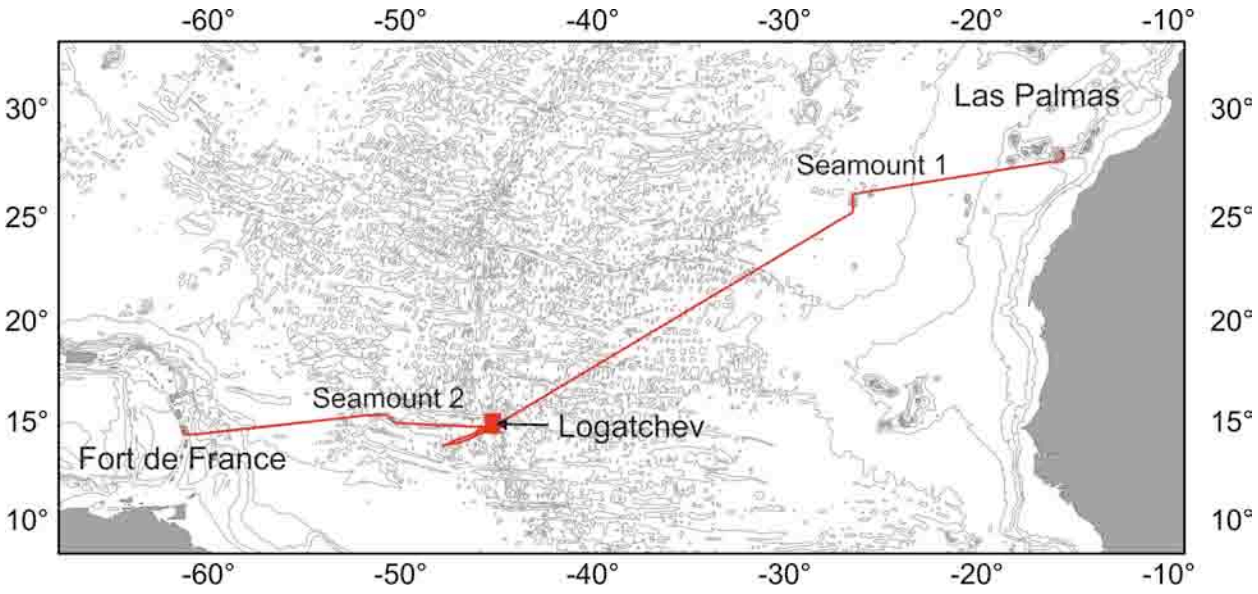

Fig. 4.1 Track chart of R/V MARIA S. MERIAN cruise MSM 10/3.

On January 17, an oceanographic mooring was deployed about 5 nautical miles from Logatchev in 4000 m water depth (Fig. 4). The 120 m long mooring was anchored on a sill between two valleys north of the Logatchev area to continuously measure the temperature, salinity, and current velocities using 5 conductivity and temperature recorders (MicroCATs) and 5 Recording Current Meters (RCMs). Recovery of the mooring is planned during a SPP 1144 cruise with the RV Poseidon in March 2009. During the first week at Logatchev (Jan. 18 – 25), twelve Ocean Bottom Seismometers (OBS) were deployed in a grid across the Logatchev vent field to record seismic activity. These will also be recovered during the Poseidon cruise in March 2009. Research work was interrupted from the evening of Jan. 18 to the morning of Jan. 20 to rescue a couple on a sailboat with a broken mast that was over 100 nm away from us. The couple abandoned their sailboat and stayed with us for the rest of the cruise. As strong winds and rough seas did not allow the deployment of the ROV, a series of CTD-rosette casts, tow-yos, and yo-yos were run to investigate how vent fluids are dispersed into the water column. MAPRs (Miniature Autonomous Plume Recorders) were attached to the CTD cable for additional information on turbidity and Eh. The first ROV dive was not possible until Jan. 25, and fluids and biota were sampled from the Irina II vent structure. During the dive, an in situ mass spectrometer (designed by Peter Girguis) was successfully deployed, providing, for the first time, online measurements of dissolved gases in vent fluids of Logatchev.

Seas were too rough for ROV deployment during most of the second week (Jan. 26 – Mar. 1) as well, so we continued our plume studies with CTD rosette casts, tow-yos and yo-yos. Hump Day was celebrated on Jan. 29 with a barbecue on the afterdeck. On March 1, the seas quieted down enough for a 2nd ROV dive, during which instruments left on the seafloor during previous cruises were recovered (the Ocean Bottom Pressuremeter and SMoni from Irina II). Mussels were collected for biological analyses, and hot vent fluids from Irina II were sampled for microbiological and chemical analyses. During the third and last week at Logatchev (Mar. 2 – 9), the CTD-rosette was deployed as during the previous weeks for plume studies. Three out of four OBSs that had been deployed during the SPP 1144 cruise to Logatchev in December 2007 with the RV L'Atalante were successfully recovered. Seas were quiet enough for ROV diving on Feb.

4, 8, and 9, and despite the limited number of dives possible during the cruise, most of the instruments that had been left on the seafloor were recovered including the Ocean Bottom Tiltmeter, the SMoni from Site B, and temperature loggers deployed in a mussel bed at Irina II. Samples for biological and chemical analyses were collected at Quest, Irina II, Site B, and Anna Louise and the in situ mass spectrometer collected data on the dissolved gases from all sampled sites. A large woodpile that had been deployed two years earlier was extensively penetrated by wood-boring bivalves, and samples were collected and brought to the ship, but no live shipworms were found. As during the previous weeks, the night program consisted of bathymetric mapping of the Logatchev vent field and surrounding areas using the ship's mulitbeam echosounder.

We began our transit to Fort de France, Martinique the evening of Feb. 9 and made a small detour en route for bathymetric mapping of a seamount at 15°20' N, 50°30' W from Feb. 10 – 11. We arrived in Fort de France as scheduled, early in the morning of Feb. 13 and were able to unload our containers and ship our airfreight by noon, despite a strike that crippled almost all of Martinique. Most of the scientific crew flew home the evening of Feb. 13, with the ROV crew flying home a day later on Feb. 14.

Summary of gear deployments / instrument usage

Gear	No. of deployments	Hours:minutes
ROV	7	46:51
CTD/Ro	21	41:32
MAPR Tow Yo	4	29:36
CTD/MAPR Tow-yo	9	59:15
CTD/JoJo	2	16:12
Moorings	1	4:12
OBS	16	5:43
EM 210	24	207:40
Sum	84	411:01

5 Preliminary Results

5.1 Bathymetric Mapping

(I. Grevemeyer)

The MARIA S. MERIAN operates a Kongsberg EM120 multi-beam echosounder. The system allows mapping with 1991 beams a stripe of seafloor, providing accurate bathymetric mapping down to depths exceeding 11000 m. This system is composed of two transducer arrays fixed on the hull of the ship that send successive frequency coded acoustic signals (11.25 to 12.6 kHz). Data acquisition is based on successive emission-reception cycles of this signal. The emission beam is 150° wide across track, and 2° along track direction. The reception is obtained from 191 overlapping beams, with widths of 2° across track and 20° along it. The beam spacing can be defined as equidistant or equiangular, and the maximum seafloor coverage fixed or not. The echoes from the intersection area (2° x 2°) between transmission and reception patterns produce a signal from which depth and reflectivity are extracted.

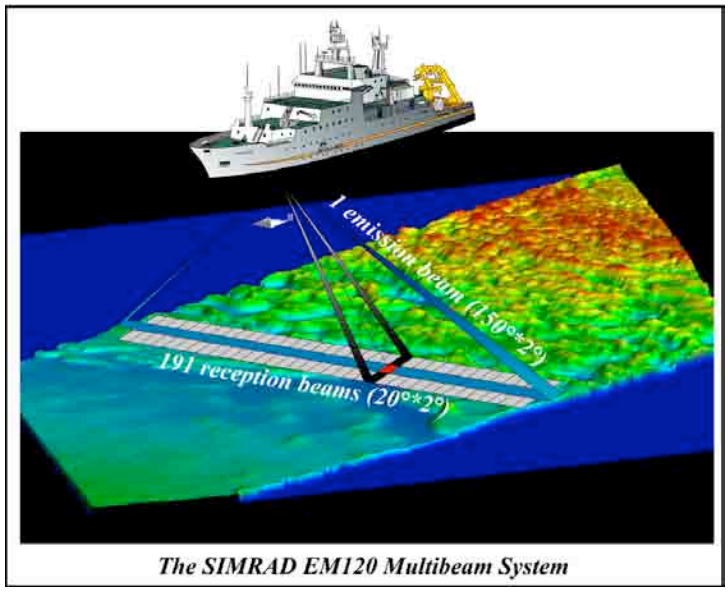

Fig. 5.1 Acquisition method for bathymetric and backscatter data from the Simrad EM120 system (crossed beams technique).

During the cruise MSM10/3 bathymetric mapping was conducted to yield the regional bathymetry in the vicinity of the Logatchev hydrothermal vent field. Further, mapping operation was scheduled for night operation and times when it was not possible to handle any other equipment, for example during bad weather conditions. Overall, the mapping program was successful, providing a detailed high resolution map of the area. Interestingly, the Logatchev field is located to the east of the neovolcanic zone and hence off-axis. Further, bathymetric mapping suggested that at the latitude of the vent field, spreading caused a highly asymmetric structure of the median valley and flanking rift mountains with profoundly higher elevations on the eastern African plate.

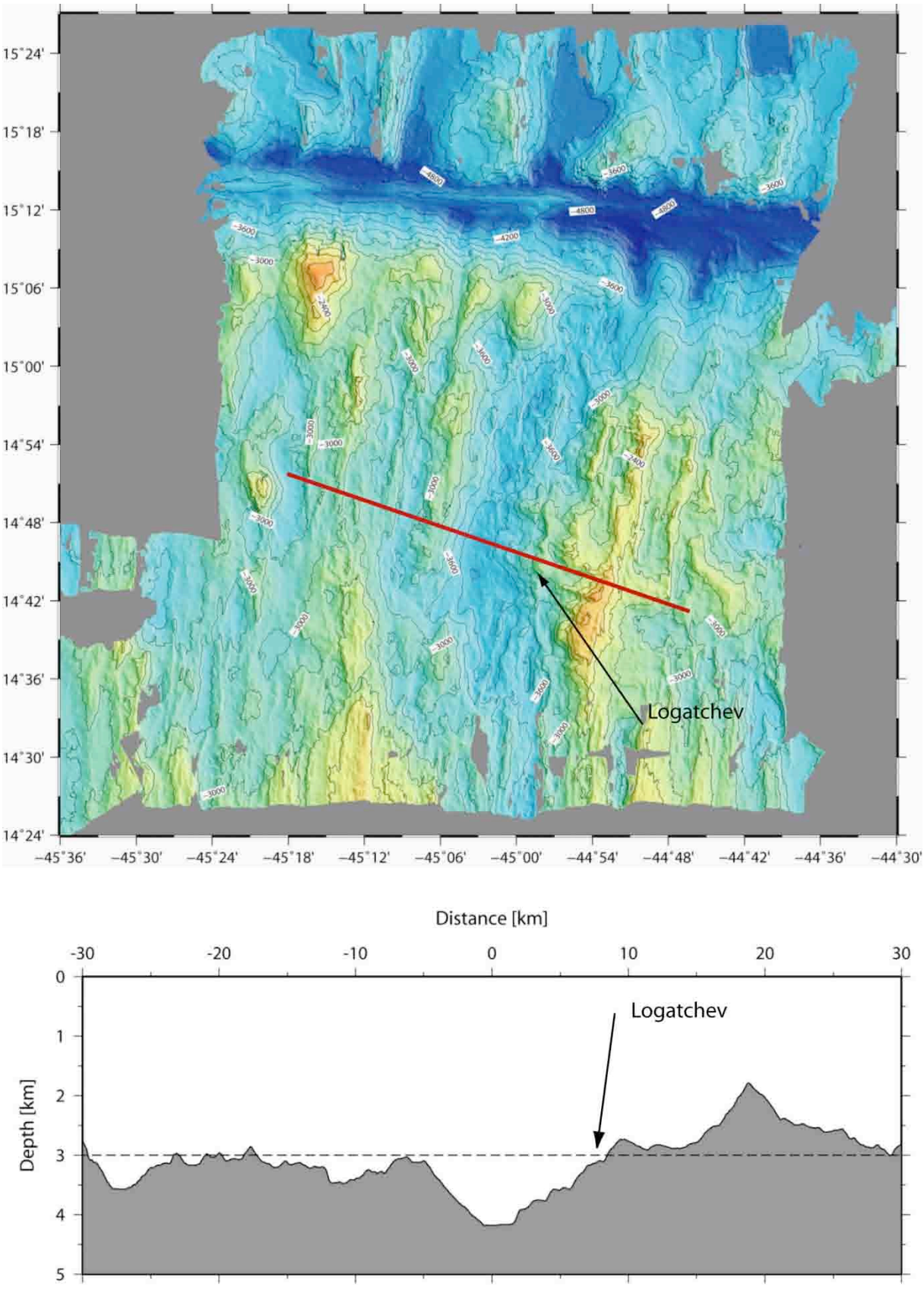

Fig. 5.2 Bathymetric coverage obtained in the vicinity of the Logatchev vent field (top). Red line marks location of bathymetric profile (bottom).

5.2 Physical Oceanography

5.2.1 CTD Measurements

(F. R. Karbe)

CTD / lowered Acoustic Doppler Current Profiling system (lADCP) casts and tow-yos were carried out between January 17 and February 8 with the CTD-rosette from the Institut für Ostseeforschung Warnemünde (IOW) that is permanently aboard the RV MARIA S. MERIAN (Fig. 5.3). We used a system configuration of a double sensor (Conductivity, Temperature, Oxygen, one Pressure sensor) Seabird SBE 911+ (SN #09P39027-0806) and a rosette holding 19 Hydrobios Niskin samplers, an lADCP system (see section 5.2.2) and a Posidonia transponder for exact positioning of the CTD. One to three Miniaturized Autonomous Plume Recorders (MAPR, provided by E. Baker, NOAA. PMEL, Seattle, USA) were attached to the rosette or the wire (for a description of the MAPR work, see 3.4.2.4). The main goal of the CTD work was to gain information on the spatial distribution of hydrothermal plumes in the Logatchev area. Water samples were analyzed for concentrations of methane and hydrogen by the gas chemistry group (see sections 5.2.4. Hydrothermal Plume Mapping, 5.3 Gas Chemistry).

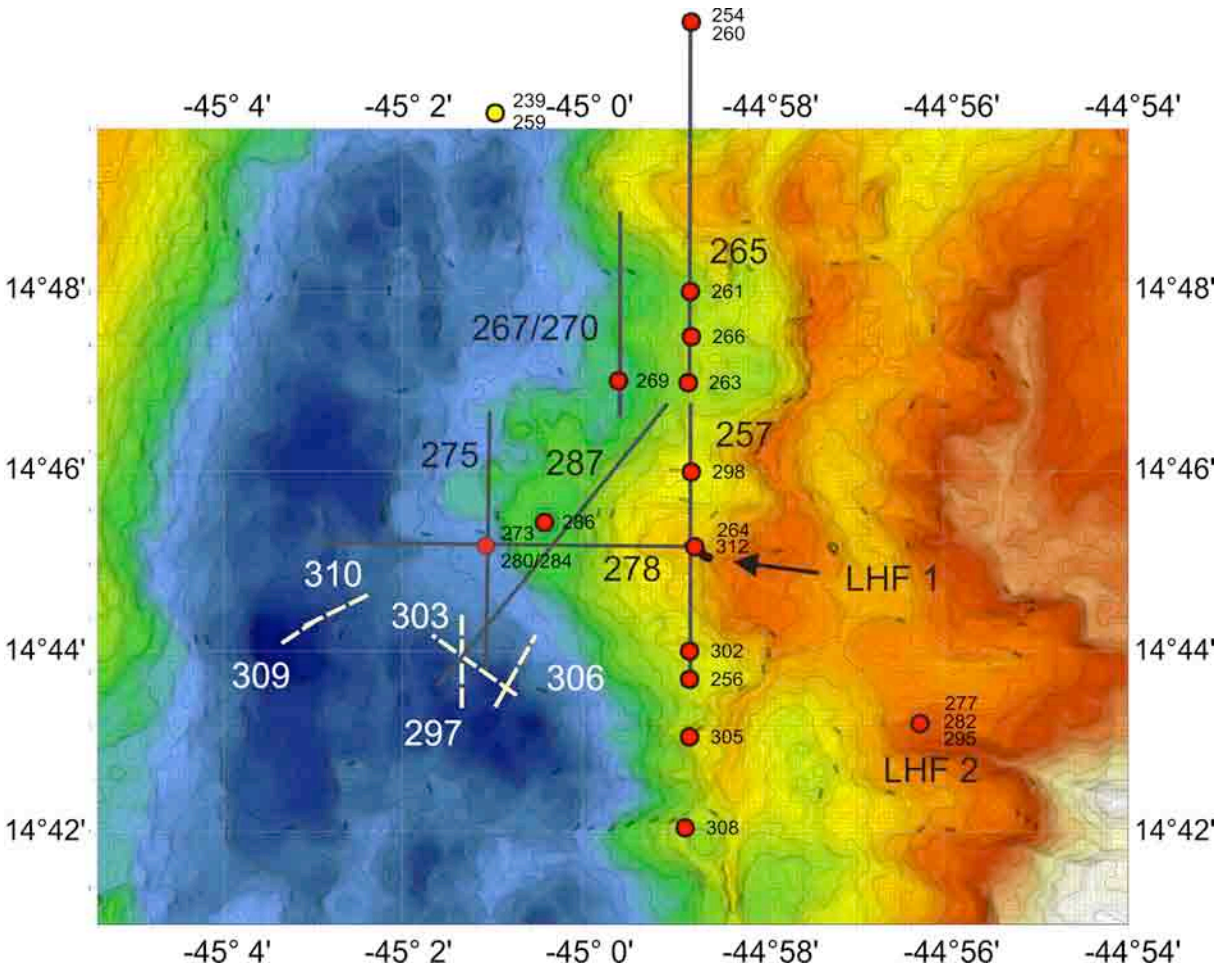

Fig. 5.3 Positions of CTD stations and tow-yows around the Logatchev hydrothermal vent area. Dots represent CTD casts, the yellow dot indicates the position of the Logatchev Mixing Mooring and associated CTD casts. Black lines indicate MAPR tow-yows spanning a depth range minimum 300 m above seafloor. White dashed lines indicate deep water tow-yos in the rift valley with a depth range of ~30-130 m above seafloor.

To measure tidal influences on a strong and deep methane signal, two yo-yo casts were carried out at the same position during a tidal cycle.

The primary CTD pump did not work properly at first and had to be exchanged. The setup of the control software caused problems initially, but after 10 casts GPS positions were available on NMEA with only two exceptions on February 3 during casts #24 and #25. Initial problems with the RMC data from the ships data base caused corrupt protocols, but this could be fixed by setting the date in the protocol to a constant which had to be changed manually every day. On February 6, station MSM-010/003-0305 ran during cross-sea conditions and winds of 6 Bft. resulting in strong rolling movements of the ship. After recovery, two Niskin bottles were damaged (one was broken, one had lost its bungee), but both could be easily fixed or replaced.

Due to the fact that post-processing and calibration of data with salinity- and oxygen-values from the water samples will be made onshore, a detailed analysis of CTD data can not be carried out until calibration of data. Oxygen concentrations (ml L^{-1}) were determined for several depths and casts, concentrations were determined by M. Perner and N. Rychlik. This data has not yet been compared in detail with the data from the two oxygen sensors. Water samples for onshore determination of salinity were taken on corresponding casts.

Data collected during research SPP1144 cruises l'Atalante cruise leg 2 in 2008 and MSM 10-3 were thoroughly inspected and calibrated. Water mass properties from both cruises clearly showed the presence of (from bottom to top) Antarctic Bottom Water (AABW), North Atlantic Deep Water (NADW), South Atlantic Central Water (SACW), Subtropical Under Water (SUW) and Tropical Surface Water (TSW). The North Atlantic Central Water (NACW) was not present around the Logatchev area (Fig. 5.4).

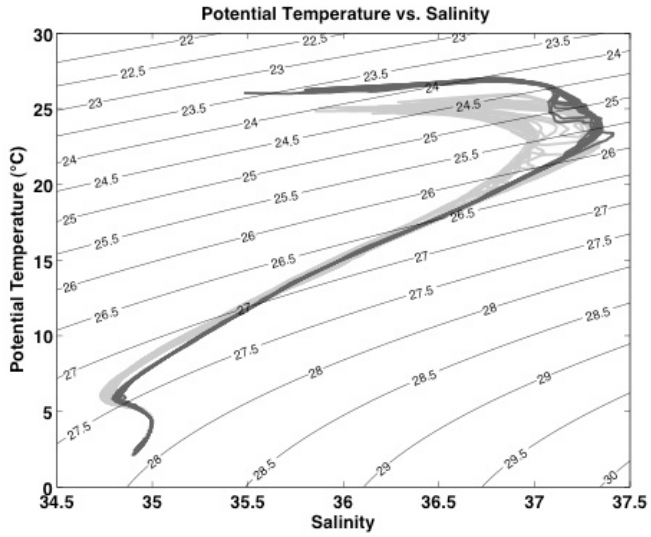

Fig. 5.4 Property-property-plot of potential temperature (ref. to zero pressure level) versus salinity, light grey depicts data collected with MSM10-3 in 2009 and dark grey data from l'Atalante cruise leg 1 in 2008.

5.2.2 Lowered ADCP

(F. R. Karbe)

Data collected by the lowered Acoustic Doppler Current Profiling system (lADCP) provided information about current velocities in the deep ocean. The system consisted of two Teledyne RDI WH 300 kHz ADCPs in a special frame that protects the instruments but does not block the

acoustic beams. A battery pack was mounted between the down looking master instrument (SN #680) and the up looking slave (SN #11461) supplying both instrument as well as being the connection point for the data interface cable. Both instruments were run with the same setup of 25 bins with 10 m bin size and single-ping mode, time between pings was 0.9 seconds. Data were processed during the cruise with the IFM-Geomar LADCP processing software including both shear and inversion methods to derive an absolute velocity profile. Time and navigation data from the ship data base were used for processing the pre-processed P-T- S-data files of the CTD casts and processed data from the ship mounted Teledyne RDI OS 75 kHz ADCP will be involved for additional processing with calibrated DTC data. The combined usage of data from navigation, CTD and vmADCP will ensure good quality of the lADCP processing.

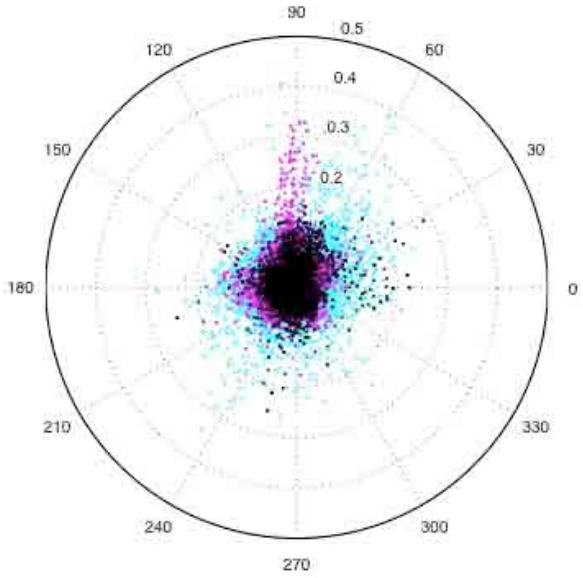

Fig. 5.5 Current magnitude and direction from MSM10-3 lADCP data for three density layers: Surface to sigma-theta 27.8581 kg m^{-3} in cyan (ca. 0 - 2500 db depth), sigma-theta [27.8582 - 27.8703] kg m^{-3} in black (plume layer, ca. 2500 - 3000 db depth) and below sigma-theta 27.8704 kg m^{-3} in magenta (deep layers below Irina II smoker). Units are degrees for direction with 90° for North and ms^{-1} for current magnitude.

Data from the lADCP additionally offered the possibility to study the influence of tides and mean currents. The mean flow field (Fig. 5.5) showed strongest influence of tides in the upper layer (see Fig. 5.5 legend for layer definition), with current maxima of up to 0.4 ms^{-1} in opposite directions. The deep layer covering most of the deep basin west of Irina II showed a clear prevailing northward movement. Plume layer velocities did not clearly show a prevailing direction, but maxima of up to 0.3 ms^{-1} from northeast to southwest were obvious. The influence of tides was probably small in velocity and confined to the patch with velocities below 0.1 ms^{-1}. However, on average all layers showed strong directional variability and current magnitudes well below 0.2 ms^{-1}.

Interannual and seasonal variability of water mass properties between the two cruises was indicated by shifts of the Antarctic Intermediate Water minimum and the surface waters. Hydrographic surveys were used to assess the spreading and dispersal of the hydrothermal plume and the mixing rates in terms of Thorpe-Scales in the lower water column. Thorpe scales were

computed following the method described by Ferron et al. (Ferron *et al.*, 1998) using potential temperature referenced to a pressure level of 2700 db. Thorpe scales and dissipation rates were estimated for each single profile (43 in total, MSM10-3 (28 profiles used) and ATA 2008 (15 profiles used)). Following vertical averaging in each profile with 25 db steps all dissipation rate profiles were averaged to obtain an average profile of turbulent diffusivity (Fig. 5.5). Similarly enhanced turbulent diffusivity occurred in a range from the depth corresponding to the upper limit the Irina II plume down to 3150 m. Above this depth range, signals did not differ significantly from background. The average turbulent diffusivity for the plume depth range is 2 x 10^{-3}, whereas for the enhanced patch it is 2.1 x 10^{-3} and the whole examined depth range 1.1 x 10^{-3}.

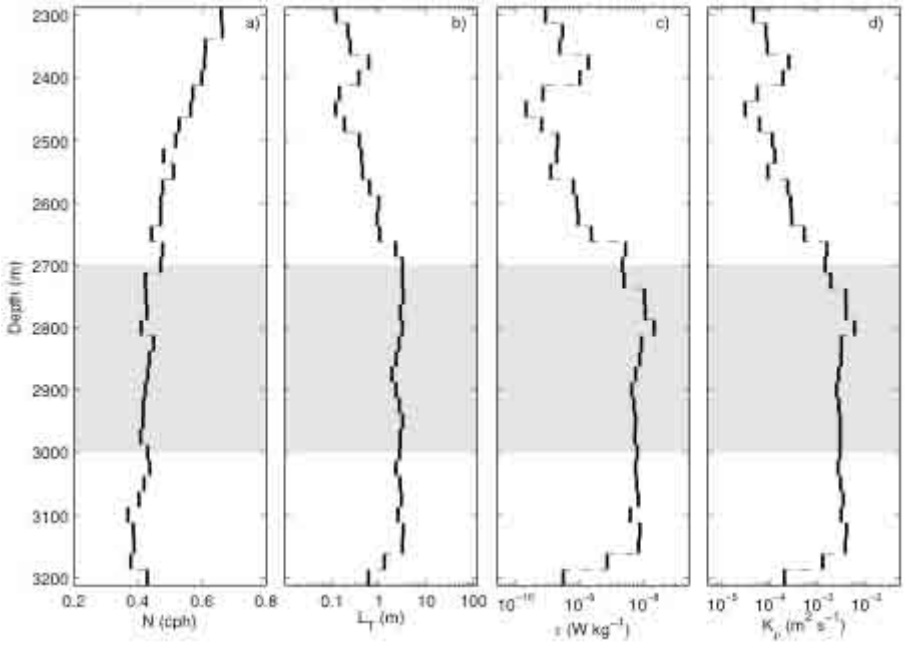

Fig. 5.6 Stratification (a), average Thorpe scale (b), average dissipation rate (c) and turbulent diffusivity (d) for all CTD casts from cruise MSM10-3 and ATA 2008 in the vicinity of Logatchev field. The depth range of the Irina II plume is highlighted in grey.

5.2.3 Logatchev Mixing Mooring

(F. R. Karbe)

On January 17, a 120 m long mooring was deployed on a sill between two depressions in the deep MAR rift valley to study mixing processes in the lower water column (Fig. 5.7). It consisted of five Recording Current Meters (RCMs) from Aanderaa (two with pressure sensors), five MicroCAT conductivity and temperature recorders from SeaBird, 18 Benthos buoyancy balls, a watchdog transmitter on top of one buoyancy ball and a releaser. The mooring was deployed anchor first and lowered to roughly 100 m above bottom where it was positioned correctly with Posidonia control and then released. The mooring will be recovered in March 2009 during Poseidon cruise POS 380.

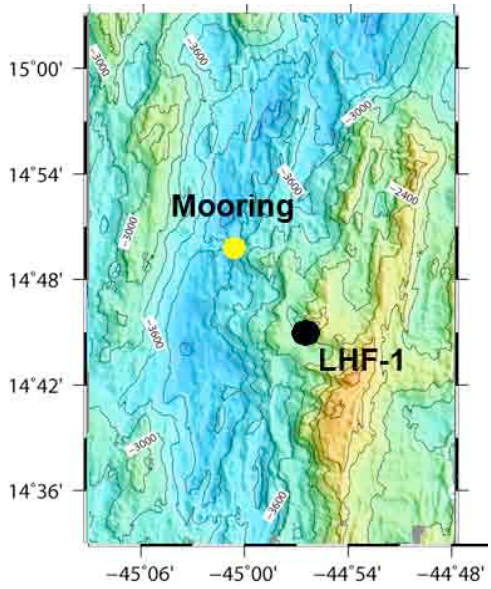

Fig 5.7 Location of the Logatchev Mixing Mooring on a sill in the deep rift valley.

5.2.4 Hydrothermal Plume Mapping

(C. Borowski)

Earlier investigations in the Logatchev area revealed that the neutrally buoyant hydrothermal plume (NBHP) above LHF-1 extends primarily in N-S direction. Turbidity signals in the water column were traced 4 km to the north and south of the LHF-1 fluid source, while W-E extension to each side was only 700-800 m. This geographical pattern is consistent with the N-S orientation of the MAR rift valley and the two-tailed expansion of the NBHP suggested that its shape is mainly influenced by N-S oriented tidal currents. Investigations during the two cruises Hydromar III and V in early and late 2007 detected stratification of the NBHP in two depth layers. The upper layer was found in 2600-2800 m water depth corresponding to 200-400 m height above seafloor in the area of LHF-1. This matches the expected height in which a NBHP rising from a 340°C fluid point source in 3000 m water depth would stratify. The second layer was consistently found in 2900–3000 m water depth, which is usually considered too deep for a NBHP fed by LHF-1 fluids. Two explanations were considered: The deep NBHP layer could represent the tongue of a plume with higher chlorinity that does not rise, but flows down slope as a “reverse plume”. However, enhanced chlorinity was not measured in fluids of any vent from LHF-1 (Schmidt et al., 2007) or LHF-2 (Fouquet et al., 2008), suggesting that none of these vents was the origin of the deep plume layer. Alternatively, the deep plume layer could originate from a yet undiscovered hydrothermal vent down slope of LHF-1. During MSM 10-3 we used time periods of weather conditions unsuitable for ROV diving for resolving this problem.

CTD-rosette stations along the same north - south transect performed during MSM 04-3 in January 2007 served for comparison of CH_4 concentrations in the water column with earlier collected data (Fig. 5.3). On the same profile, we performed tow-yos with Miniaturized Autonomous Plume Recorders (MAPR, provided by E. Baker, NOOA/PMEL, Seattle, USA) in 50 m - 450 m above seafloor (stations 257, 265). The MAPRs were attached to the CTD-rosette and occasional closing of Niskin samplers during the tow-yos served for additional samples for methane (CH_4) determinations. More tow-yos were performed west and northwest of LHF-1 in

areas of deeper waters (stations 267, 270, 275, 278, 287). While these CTD-rosette casts and MAPR tow-yos primarily served for detecting plume signals that might indicate the presence of a yet unidentified point source of super hot hydrothermalism, the strategy in a later phase of the cruise changed to searching deeper in the rift valley for diffuse fluid sources (Fig. 5.3: CTD-rosette stations 273, 280, 284, 287, MAPR tow-yo stations 297, 303, 306, 309, 310). These deeper tow-yos concentrated on a depth range of ~30-130 m above seafloor where we searched for temperature and Eh anomalies from low temperature fluid sources.

Analyses of CH_4concentrations and turbidity signals along the N-S transect confirmed earlier data. Methane concentrations were highest above LHF-1 and there was no other maximum which would indicate an additional CH_4 source north or south of LHF-1 (Fig. 5.8). A maximum of 490 nmol L^{-1} CH_4 above LHF-1 suggested that the center of the NBHP stratified in 2750 m water depth. While this value was higher than the maximum CH_4 concentration measured in early 2007 (Keir *et al.*, 2009), diluted CH_4 spread less far to the north and south.

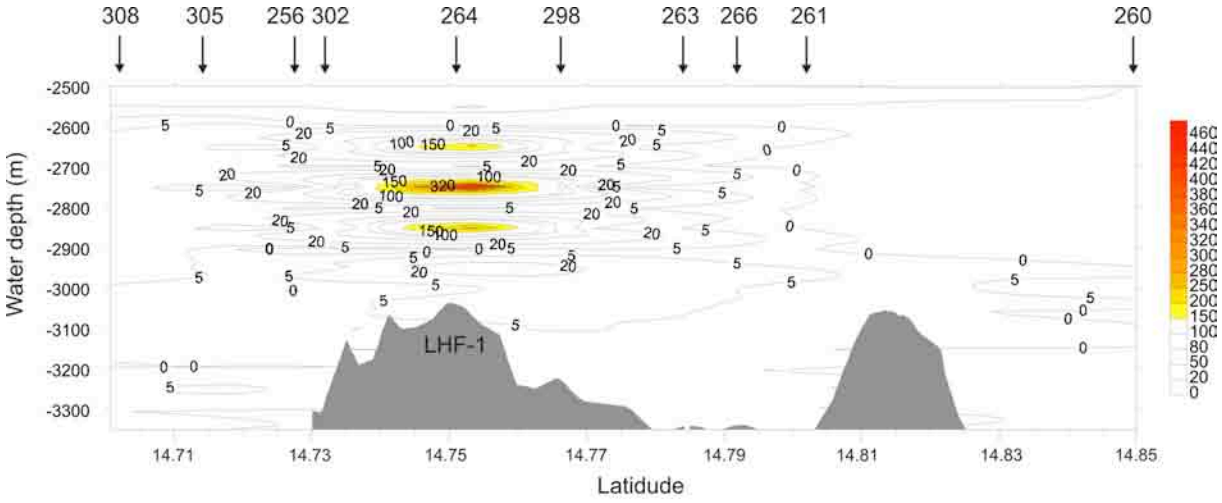

Fig. 5.8 Methane concentrations (nmol L^{-1}) in the water column between 2500 m and 3300 m water depth on a N-S directed transect across LHF-1. Arrows indicate positions of individual CTD-rosette deployments (see also Fig. 5.3).

Turbidity signals recorded with MAPRs confirmed the center of the NBHP in 2750 m water depth above LHF-1, and these data suggested a major extension of the NBHP to the north (Fig. 5.9). Similar to earlier investigations, a deeper plume layer was observed in 2900-3000 m water depth (see tow-yo 257 in Fig. 5.9), but the MAPR tow-yo stations 267, 270, 275 and 278 west of the N-S transect did not reveal turbidity signals or differential redox potential that would indicate an additional hot fluid source. An occasional observation during tow-yo station 278 of up to 0.005 ΔNTU in 3050 m water depth and at similar potential temperature as the deep plume layer above LHF-1 suggested that NBHP tongues may indeed descend down slope with water layers following the bottom morphology (Fig. 5.10).

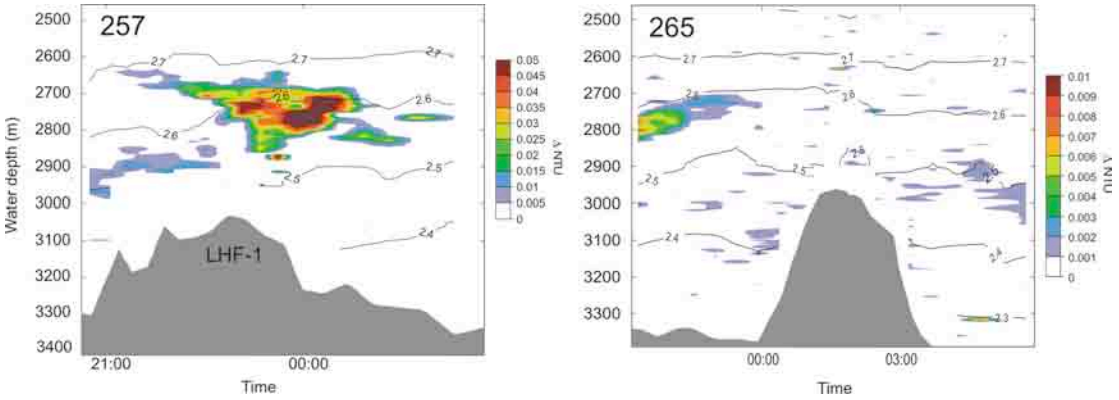

Fig. 5.9. Turbidity signals of the buoyant hydrothermal plume (as differential nephelometer turbidity units, ΔNTU) recorded by MAPR tow-yo stations 257 and 265 in S-N direction (see Fig. 5.3). Contour lines show isotherms of potential temperature.

While these results did not indicate the presence of another hot fluid source west or north of LHF-1, a number of CTD-rosette casts during this and earlier cruises revealed methane concentrations exceeding background values at water depths deeper than 3000 m suggesting that diffuse fluid sources may exist in deeper areas (Fig. 5.11; see also compilation plot in Appendix with all observations of elevated CH_4 concentrations above background levels in >3000 m water depths during SPP1144 cruises in the Logatchev area). The highest CH_4 concentration we observed was obtained in 3800 m depth with CTD cast station 273 that was located at a position at which elevated CH_4 values were measured during SPP1144 cruise M 64-2. We performed CTD cast stations 280 and 284 as yo-yos at the same position in 2500-3900 m depth. The duration of the yo-yos was 6 and 8 h at different day times to evaluate possible tidal influence on the presence of CH_4. Niskin bottles were closed approximately every 30 minutes in various depths, but none of the 38 samples contained CH_4 concentrations significantly above background (Fig 5.11) suggesting that plumes of elevated CH_4 occur only sporadically.

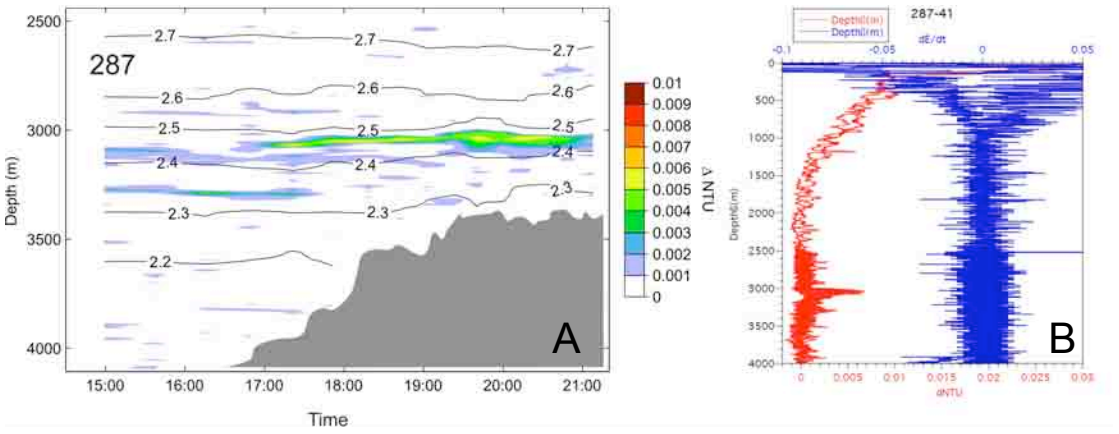

Fig. 5.10 Station 287 MAPR. A: Turbidity signals of the buoyant hydrothermal plume (as differential nephelometer turbidity units, ΔNTU; note different scale than in Fig. 5.9) recorded by MAPR tow-yo station 287 in SW-NE direction (see Fig. 5.3). Contour lines show isotherms of potential temperature. B: Turbidity (ΔNTU, red) and differential redox potential (ΔEh/Δt, blue) of entire tow-yo against depth (graph provided by E. Baker). Note ΔEh/Δt spike at 3900 m.

Fig. 5.11 CH_4-concentrations measured during MSM 10-3 in deep waters of the rift valley east of Logatchev. Left: examples for elevated CH_4 concentrations in deep tow-yos. Right: CH_4 not significantly different from background in CTD yo-yo stations 280 and 284.

A significant Eh anomaly encountered at the beginning of tow-yo station 287 in 3900-4050 m water depth suggested the presence of reduced compounds in bottom-near waters in the rift valley which might be associated with a diffuse fluid source (Fig. 5.12; see also Fig. 5.10B). Deep tow–yo station 303 across that position revealed CH_4 concentrations well above background (Fig. 5.11). Samples from other tow-yo profiles in the deep rift valley sporadically brought up slightly elevated CH_4 concentrations, but an Eh anomaly was never again observed, and we therefore were not able to localize a source of diffuse fluids.

Fig. 5.12 Eh anomaly close to the seafloor in the rift valley. The constant rising of mV signals before 16:27 and after 16:30 reflects the usual drift of the sensor, while the steep drop between these two time points and measurements is considered a true drop of the redox potential.

Conclusions

We were able to trace neutral buoyant hydrothermal plume in several kilometers distance from LHF-1, but our data do not support the presence of other focused hydrothermal vents within this distance range down slope of LHF-1. The deeper layer of the NBHP around LHF-1 most likely represents a recurrent tongue of plume that descends with waters following the slope morphology. Methane was measured in the deep rift valley, but its occurrence is sporadic and not reproducible by CTD casts or CTD/MAPR tow-yos. The observation of a redox potential anomaly close to the seafloor in the rift valley suggests that the methane may come from diffuse outflow. However, methane and redox potential anomalies could be influenced by tidal currents

and perhaps also by tidal effluent pulses which impede localization of the sources by CTD casts and MAPR tow-yos.

5.3 Gas Chemistry

(M. Warmuth, A.Heddaeus)

Introduction

Due to bad weather conditions the main objective of the work during MSM 10-3 was to localise and characterise hydrothermal plumes using in situ sensors (CTD attached with MAPRs. for further description see section 5.2.2), and on board analytical techniques to determine concentrations of dissolved reactive gases (CH_4, H_2). To elucidate the transformation of carbon species and reduced gases in the hydrothermal fluids, a comprehensive set of samples (146) was fixed for on shore analysis of stable isotope contributions (H and C) of fluid components. Also different hydrothermal fluids (hot and diffuse), that were taken during the ROV dives, were analyzed.

For this purpose 32 stations were covered by CTD-rosette and a total of 365 water samples were obtained from these CTD stations and 5 ROV stations. The CTD was either used for a normal up- and downcast, tow-yo and yo-yo profiles. For ROV dives, samples were obtained with the KIPS (see section 5.4)

In addition, hydrogen was monitored in incubation experiments conducted by M. Perner (Uni Hamburg), C. Huang (MPI, Bremen) and D. Fink (MPI, Bremen) on the metabolism of microorganisms present in hydrothermal fluids (Section 5.6.1), sediments (Section 5.6.2) and mussels (Section 5.7).

Samples and Methodology

For on board measurements of dissolved methane and hydrogen up to 600 ml of sample was connected to a high grade vacuum using a technique modified from the method described by Schmitt et al. (1991). Aliquots of the released gas were transferred via a septum from the degassing unit into the analytical system. A gas chromatograph (THERMO TRACE) equipped with a packed stainless steel column (Molecular sieve 5A, carrier gas: He) and a pulsed discharge detector (PDD) was used to separate, detect and quantify hydrogen. Recording and calculation of results was performed using a PC operated integration system (THERMO CHROM CARD A/D). Analytical procedures were calibrated daily with commercial gas standard (LINDE).

CO, CO_2, and CH_4 concentrations of extracted gas were determined using a gas chromatograph (CARLO ERBA, 8000 top). Between 0.1 to 1 ml of gas was injected on and separated by a 10 mm long packed column, passed a thermal conductivity detector to a methanizer transforming all oxidized carbon species into CH_4 which then was quantified by a flame ionization detector. Data were recorded for both detectors by a PC based commercial integration software. Carrier gas was helium, oven temperature was 3 min isotherm 60°C, 40°/min to 120° kept for 10 min.

Samples for the determination of $\delta^{13}C$ of the dissolved light hydrocarbons were obtained by degassing the water samples with a vacuum technique (see above). Aliquots of the released gas were transferred via a septum from the degassing unit into gastight glass vials filled with NaCl-

saturated water for later on shore analysis by GC-Isotope-Ratio-Mass-Spectrometry. Afterwards the septum was sealed with silicone on the outside.

Preliminary Results

For the working area, the known plumes above the Logatchev hydrothermal fields (LHF-1 and -2) showed clear imprints of hydrothermal activity within the water column by anomalies in the methane and hydrogen contents. These anomalies were present at a water depth from 2300 to 3050 m. Over the main Logatchev field, elevated concentrations of both hydrogen and methane over a certain depth range clearly indicated the hydrothermal plume (Fig. 5.13). The maximum values of 1960 nM and 490 nM for hydrogen and methane respectively, were measured at a depth of 2720 m.

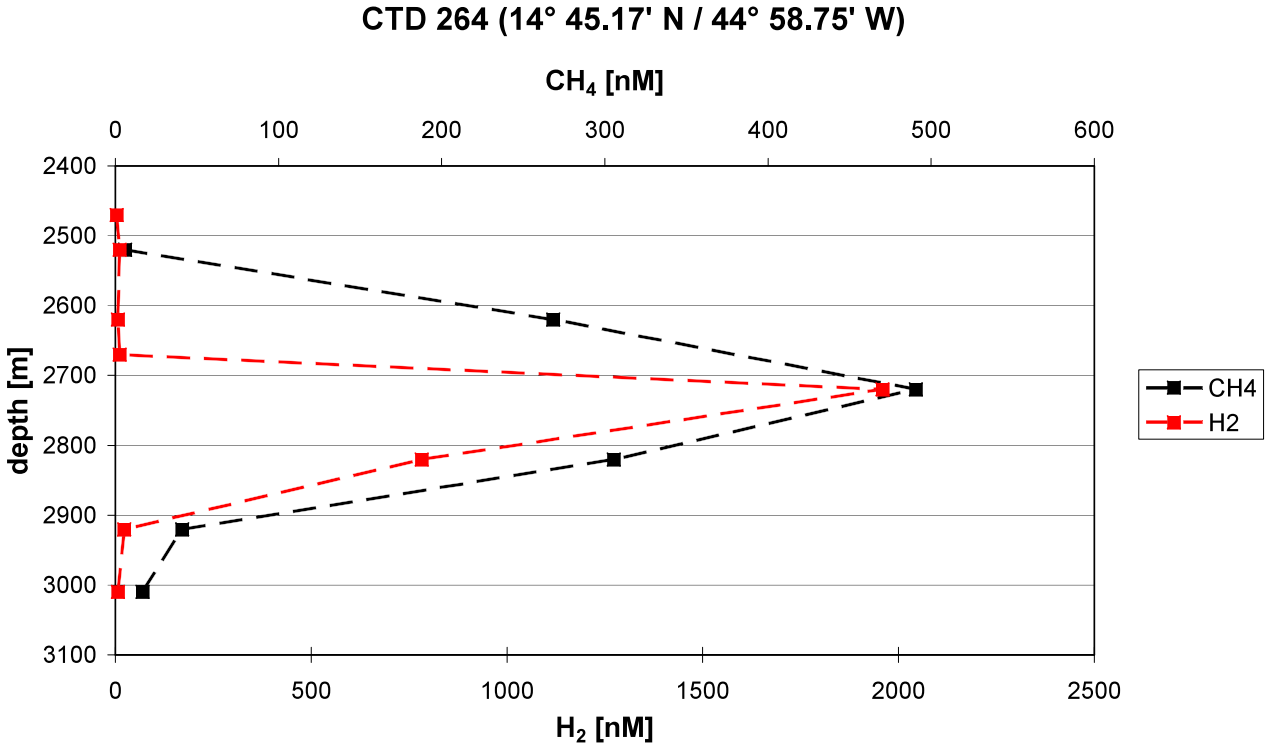

Fig. 5.13 Concentrations of H2 and CH4 over the main Logatchev field.

However, such clear indications were only measured in a few analyzed hydrocasts. Unfortunately, an online sensor indicating the hydrothermal plume was not available. Therefore, sampling the right depth or area was very difficult. Figure 5.14 shows that we found evidence for plumes at depths down to 4150 m. With the main Logatchev field at a depth of around 3000 m, this indicated that there could be a source lying even deeper. But with our limited possibilities we were not able to detect the source. The deep source showed values of up to 31 nM hydrogen and 87 nM methane.

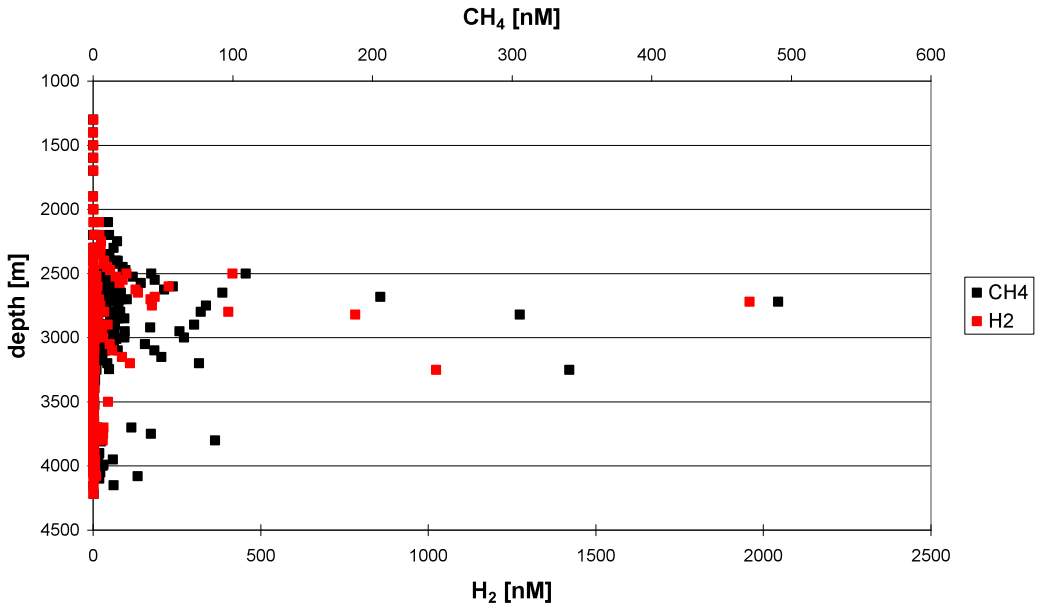

Fig. 5.14 Concentrations of CH_4 and H_2 in water samples of all CTD stations.

Samples obtained by the ROV directly at the fluid emanations revealed very high concentrations of dissolved hydrogen and methane. Maximum concentrations found in hot fluids reached up to 3.2 mM and 2.2 mM of hydrogen and methane respectively. In diffuse fluids, maximum concentrations reached up to 0.72 mM and 0.26 mM of hydrogen and methane.

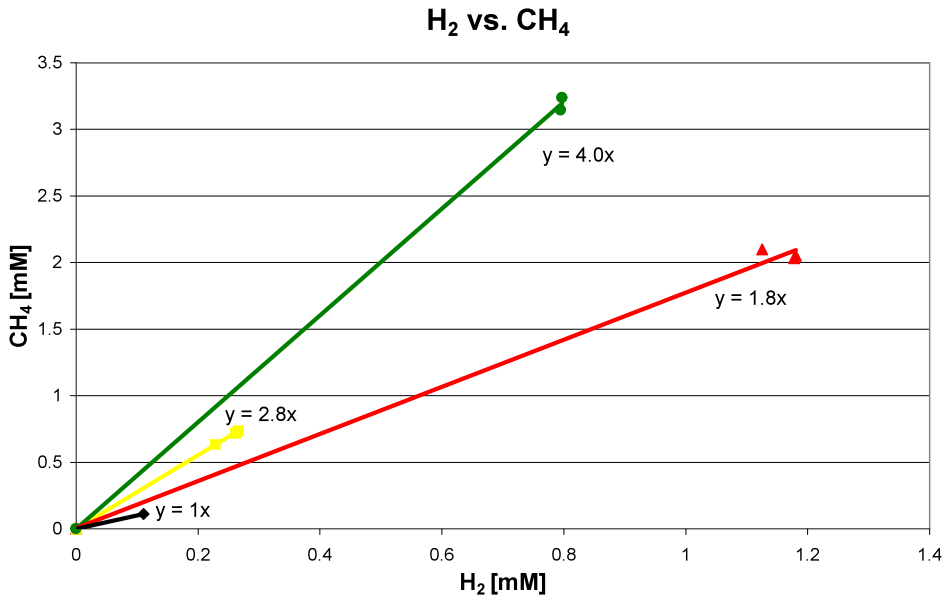

Fig. 5.15 H_2 vs. CH_4 ratios. Green: hot fluids from "Anna Louise", Yellow: mussel bed at "Irina II", red: "Microsmoker"; black: mussel bed at "Irina II"

As shown in Fig. 5.15 we never found high hydrogen vs. methane ratios of about 5.7 as reported by Charlou *et al.* (2002) from the ultramafic Rainbow vent field and by former HYDROMAR cruises to Logatchev. The highest ratio we measured was about 4.0 in the hot fluids from a chimney near the "Marker 30" at the "Anna Louise" smoking crater.

5.4 Fluid Chemistry

(D. Garbe-Schönberg, P. Hach, V. Klevenz, M. Peters

5.4.1 KIPS (Kiel Pumping System) Analyses

Objectives for the work of the fluid geochemistry group were (i) to learn about temporal variability of the elemental and isotopic composition of Logatchev-1 hydrothermal fluids through continuation of our time series study covering 6 years and comparison to data from 1996 (Douville *et al.*, 2002), and through sampling on shorter time scales during tidal cycles; (ii) to identify spatial heterogeneity between different vent sites, and on the decimeter scale within a mussel field; (iii) to compare Logatchev-1 to other hydrothermal systems in serpentinized areas, especially to the phase separated system Logatchev-2; (iv) to focus investigation on metal complexation and mechanisms of detoxification; (v) to study the hydrothermal geochemistry of elements like Ti that have not been analysed so far. Bad weather conditions allowing a very limited number of ROV dives led us to include the search for known and inferred hydrothermal plumes with CTD-tow yos into our sampling schemes.

The ROV-based fluid sampling system "KIPS" (Kiel Pumping System, KIPS-3) was used during the entire cruise for sampling of both diffuse warm and focused hot fluids. Compared to previous cruises, the design of the KIPS system was significantly modified with the objective to (1) improve the tightness of sample containers and avoid gas-induced leakage of samples causing cross-contamination of gases; (2) develop a more compact, self-contained unit which can easily be mounted and dismounted on the ROV tool sled; (3) use a deep sea peristaltic pump for *in situ*-fixation by adding reagents into a sample container; (4) use a combination of different temperature sensor technologies to improve accuracy of temperature data. The new KIPS fluid sampling system was successfully tested and used during this cruise. Minor difficulties with the mounting of the actuator driving the valve could be fixed. A more detailed description of the system components is given in the Appendix. In addition to the KIPS, four titanium syringes ("Majors" after von Damm et al., 1985, manufactured by IFREMER/ BREST-MECA) were prepared to collect hot hydrothermal fluids (see Appendix for details). Due to shortage of both diving time and space on the ROV these samplers were not used.

On-board measurements included pH, Eh, concentrations of oxygen, sulfide, Mg, Cu, Zn, and Pb. Analyses were performed to ascertain the quality of sampled hydrothermal fluids (i.e., the degree of admixed seawater) and to provide an initial characterization of fluid composition. Details of on-board sub-sampling and sample preparation as well as analytical methods used are summarized in the Appendix. For the first time, sulfide could be analysed from samples with *in situ*-fixation immediately after sampling on the seafloor allowing a more accurate quantification of dissolved H_2S.

5.4.2 In Situ Temperatures and Chemistry of Logatchev-1 Hydrothermal Fluids

Irina II Microsmoker. The small black smoker chimney "Microsmoker" SE to the Irina II complex was sampled during station 290 ROV (dive #44) with the SMoni temperature logger still in place. The chimney orifice was hidden by black smoke during sampling and we were not able to sample the maximum vent temperature and pure undiluted fluid. Fluid samples were blackened from "smoke" particles that originated from mixing with seawater. Significant entrainment of seawater was also reflected in elevated Mg concentrations as well as in a range of

pH values from 3.79 to 6.25 (Tab. 5.1) and the average temperature of only 321 °C that was recorded during sampling (Fig. 5.16). The short maximum temperature reading of 351.4 °C was in the range measured in the years before: 367 °C in 2008 (ROV *Kiel6000*, ATA 1), 340 °C in 2007 (ROV *Jason*, MSM 04) (Tab. 5.2). Dissolved H_2S was up to 1.0 mmol/L as determined from untreated original fluid samples after recovery (Tab. 5.1). This sulfide concentration compares to 0.95 mmol/L measured in 2005. All these concentration values are not endmember-corrected yet.

Site "B". The smoking crater site "B" was visited during station 313 ROV. After recovery of the long-term temperature logger "SMoni" from chimney "B4" this orifice was sampled at an average temperature of 350.6 ± 0.4 °C. The maximum temperature measured was 352.3 °C, comparing to 363 °C in 2008 (ROV *Kiel6000*, ATA 1), and 343 °C in 2007 (ROV *Jason*, MSM 04) (Fig. 5.16, Tab. 5.2). Values between 3.99 and 4.75 pH were determined in these samples. The sulfide concentration of up to 1.2 mmol/L for Site B was clearly lower than in 2005 (3.6mmol/L) and 2007 (3.3mmol/L). This was possibly caused by a lower fluid fraction in the sample.

Anna Louise. The small chimney with Marker #30 (and burnt plastic lid marker) atop the rim of the smoking crater "Anna Louise" was resampled during station 315 ROV. Temperature readings were very stable at 350.6 ± 0.5 °C and maximum at 352.4 °C (Fig. 5.16). For comparison: 352 °C were recorded in 2008 (ROV *Kiel6000*, ATA 1), and 349 °C in 2007 (ROV *Jason*, MSM 04). The measured pH values (*ex situ*) displayed an unexpected range of 3.96 – 5.25 pH. Sulfide determined in original, untreated samples on-deck was determined to 1.1 mmol/L, comparable to 0.9 mmol/L measured in 2005.

Irina II diffuse fluids from mussel fields. Typically, temperatures recorded in mussel fields ranged from 3 to 30 °C (Figs. 5.17, 5.18). The voltammetric determination of dissolved Zn, Cd, Pb, and Cu yielded highest values for Zn (171 – 1009 nM), followed by Cu (13 – 169 nM). Lead was detected in five of seven analysed samples, with concentrations between 1.9 and 4.3 nM (Tab. 5.1). Cadmium was below detection limits in all samples. A correlation of these metal concentrations with temperature (for these samples between 5 and 13.8°C) and pH (6.54 – 6.94) was not visible, thus it appears that they are not governed by the degree of fluid dilution. Concentrations of dissolved sulfide in diffuse fluids from Irina II were clearly lower than in hot fluids from Irina II (Microsmoker), Site B and Anna Louise because of a much higher seawater contribution. Sulfide concentrations for diffuse fluids ranged between 1.0 and 26.4 µmol/L H_2S.

At the site Anna Louise the first *in situ*-fixation of dissolved H_2S from a hot fluid succeeded. The *in situ* sample displayed a four times higher concentration value (4.4 mmol/L) compared to the maximum concentration value of other fluid samples taken at the same site (1.1 mmol/L). The latter samples reacted with ZnAc only after recovery on board. The clear difference in the sulfide concentration of both types of samples indicates that a significant loss of sulfide in the time span between fluid sampling and fixation on board must occur. Thus, *in situ* sulfide fixation is a new proper tool to determine concentration values of dissolved H_2S that are not distorted by oxidation processes during sampling and the ascent of the ROV to the surface. Moreover, the successful application of *in situ*-fixation at other vent fields will allow recalculation and reinterpretation of sulfide concentration data generated during the past years. This will provide a better view of the sulfur cycle at hydrothermal systems.

Table 5.1 Results from on-board chemical analyses and measured data.

Stat. No.	description	Sample ID	bottle	Date	T (°C)	pH	Eh	H2S (µM)	Mg (mM)	O2 (µM)	Zn (nM)	Cu (nM)	Pb (nM)
272 ROV	Irina 2, diffuse	3	A1	25.01.2009	9.7-11.8	6.56	-87	15.3	49.5	152.08	171	13	b.d.l.
		4	A2		13.7-15.6	6.65	-107	15.2	53.5	164.66			
		5	A3		13.8	6.69	-50	1.6	53		488	49	4.3
		6	B4		13.8	7.43	181			220.51			
		7	C9(ZnAc)		13.8			26.4		293.94			
		-	C8			6.7	-75	7.3	50		275	16	b.d.l.
290 ROV	Irina2, Microsmoke r	9	A2	01.02.2009	130-160	6.25	-160	2.3	46				
		10	A3		215	5.36	-240	144.6	31	58.73			
		11	B4		352	3.76	-256	973.1	12	(A3+A4)			
		12	B5		320-330	4.17	-275	1030.5	15				
300 ROV	Irina 2, diffuse, mussel patch	16	A2	04.02.2009	6.6	6.94	-192	2.5	52	234.58	199	169	2.9
		17	A3		6.5	6.9	-149	3.1	51	229.75	219	36	1.9
		18	B4		6.6	7.1	-133	1.0	51.5	235.80	(above mixed sample A2-B6)		
		19	B5		10.2	6.98	-152	1.7	52	209.00	214	47	2.8
		20	B6		7.0-11.3	6.81	-149	5.1	52	217.06	(above mixed sample B5-C7)		
		21	C7		7	6.85	-179	4.9	51	207.90			
		22	C8		22.2	6.63	-175	7.1	49	171.40			
		23	C9		5	6.54	-200	5.7	49.05	177.99	1009	80	3.9
313 ROV	site B	11	A2	08.02.2009	350	4.75	-231	160.8	14.5				
		12	A3		350	3.99	-208	915.8	8				
		13	B4		350	4.44	-170.1	1231.1	16.5				
		14	B5		350	7.85	positive	696.1					
315 ROV	Anna Louise, hot	14	A1(ZnAc)	09.02.2009	352			4350.1	36.5				
		15	A2		352	4.93	-151	920.6	16.5				
		16	A3 (gas)		350	4.9		758.2					
		17	B4		330	5.25	-265	557.6	21.5				
		18	B5		330	4.3	-190	1083.0	16.5				
		19	B6		330	3.96	-220	624.5	11.5				

Tab. 5.2 Measured temperatures of hydrothermal fluids venting from black smokers

Area	*Site*	*2008* T_{max} *(°C)*	*2009* T_{max} *(°C)*	*2009* T_{avg} *(°C)*	*Fluid sample No.*
(A) Black smokers					
Irina II	Microsmoker	367	351.4	321 ± 31	290 ROV-09, 290 ROV-10 290 ROV-11, 290 ROV-12
Site "B"	B4	363	352.3	350.6 ± 0.4	313 ROV-10, 313 ROV-11 313 ROV-12, 313 ROV-14
Anna Louise	Chimney @ Marker #30	352	352.4	350.6 ± 0.5	315 ROV-13, 315 ROV-14 315 ROV-15, 315 ROV-16 315 ROV-17, 315 ROV-18 315 ROV-19

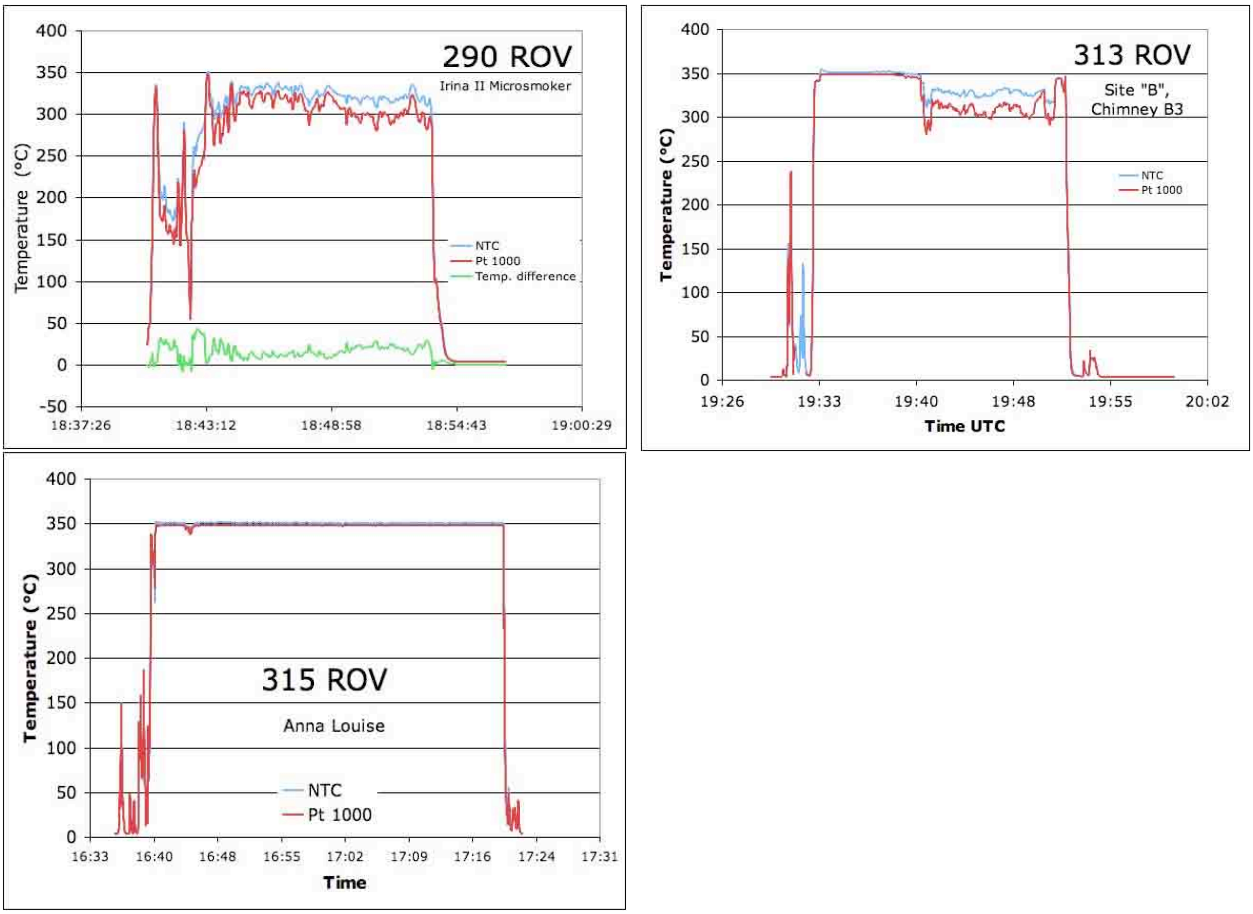

Fig. 5.16 Temperature readings during KIPS sampling of hydrothermal fluid venting from black smokers at Irina II (290 ROV), Site "B" (313 ROV), and Anna Louise (315 ROV).

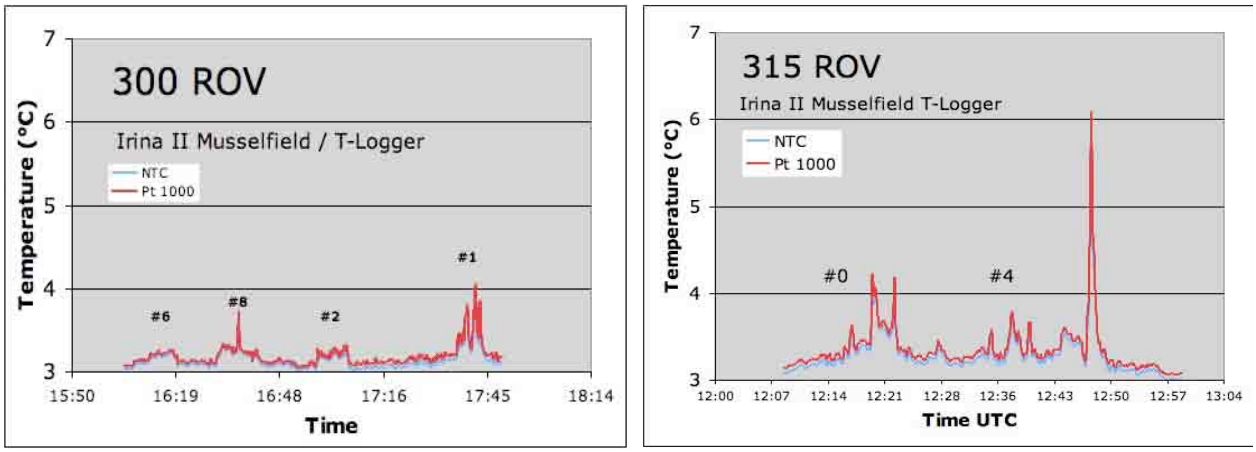

Fig. 5.17 Temperature readings in diffuse fluids of the large mussel field S of the Irina II complex, at six sites of temperature loggers #0 - #8 (stations 300 ROV, 313 ROV).

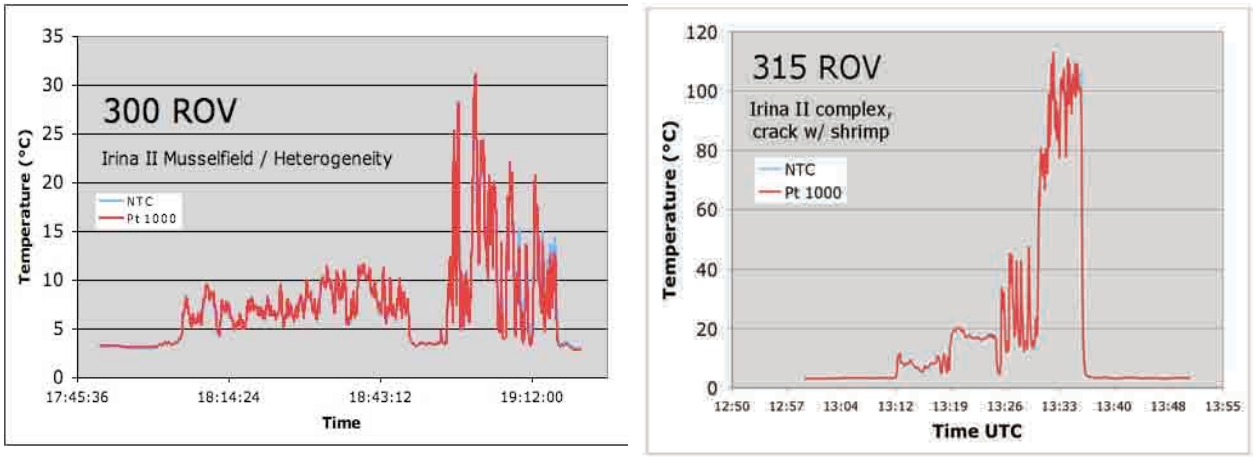

Fig. 5.18 Temperature readings in diffuse fluids at the site of a heterogeneity experiment, mussel field close to the base of Irina II complex (300 ROV). Fluids seeping from a crack in beehive smokers at the Irina II complex, with abundant shrimp and mussels (315 ROV).

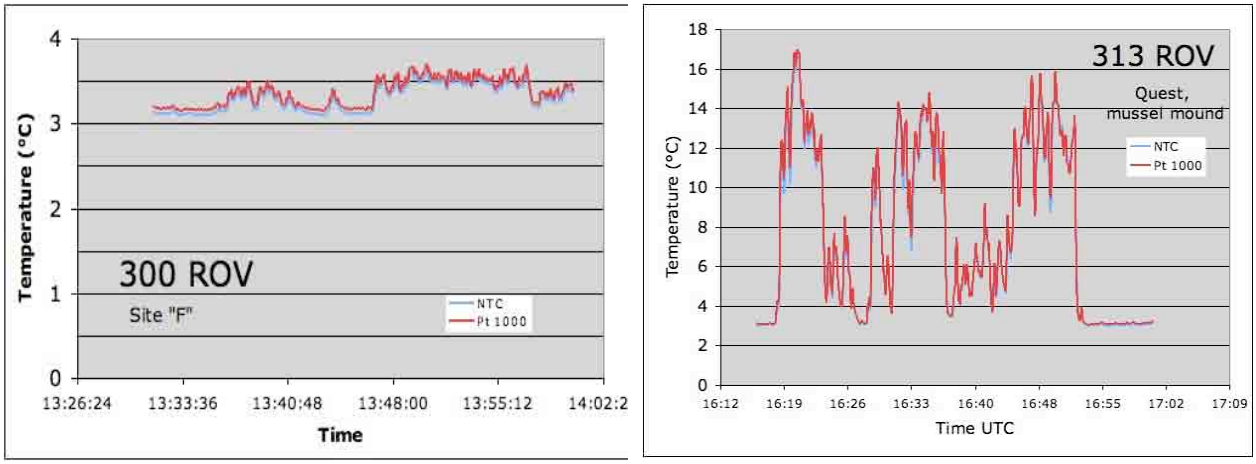

Fig. 5.19 Temperature readings above bacterial mat where push cores were taken (300 ROV). Diffuse fluids in "mussel mound" sampled at the Quest site (313 ROV).

Only very limited conclusions can be drawn from the data generated on board ship. Both temperature readings and sulfide concentration data for hot fluids from black smokers suggest that significant changes in the temperature regime have not occurred during the last years. The activity of black smokers in the Logatchev-1 hydrothermal field appears to be very stable over a time span of 6 and 13 years, respectively. This is in apparent contrast to observations at the Irina-II complex where hydrothermal venting has been waning over the last 2-3 years. Dramatic changes in mussel colonization patterns of mussel fields and the Irina II complex suggest that the local fluid regime at this site must have changed significantly. However, insight into more subtle changes in chemical composition can only be achieved after analyses in the home laboratories have been completed. Our analytical approach comprises a wide array of analytical techniques for measuring the concentrations of major, minor and trace elements and the isotopic compositions for selected elements (Ca, Sr, Cl, Hf, S, C, H, O) in the hydrothermal fluid. The ultimate goal is a quantitative characterization of fluid composition that will represent the base for balancing the mass flux from mantle to ocean.

5.5 In Situ Gas Measurements by Mass Spectrometry

(S. Hourdez)

The in situ mass spectrometer (ISMS) was deployed on all dives and performed well. The water is pumped from a nozzle mated to the KIPS nozzle and a temperature probe. After going through some length of tubing and a cooling coil, the water flows over a Teflon membrane to let gases pass into the mass spectrometer. In-line and downstream of the system, a pH probe records data throughout the dive.

During these dives, measurements were made on:

- diffuse fluids surrounding mussels (with or without visible shimmering water)
- water overlying a bacterial mat
- hot fluids (temperature up to 352˚C)

Quantification will require calculations back in the laboratory and only rough values or trends are reported here.

Overall view

Concentrations ranging from micromolar to millimolar values were measured in situ with the system. In general, the CH_4/CO_2 ratio remained constant for all fluids measured. However, the H_2/CH_4 ratio suggests that there is proportionately less hydrogen near mussels than in the hot fluid and the point source of shimmering water where no mussels were found (see diffuse areas below).

The different fluids have different H_2 to temperature relationships (Fig. 5.19), including a focused shimmering water emission compared to Microsmoker chimney, only a few meters away. This may indicate different fluid sources or a single fluid source and different extent of conductive cooling for some points of emission. This will require more detailed analyses of the data.

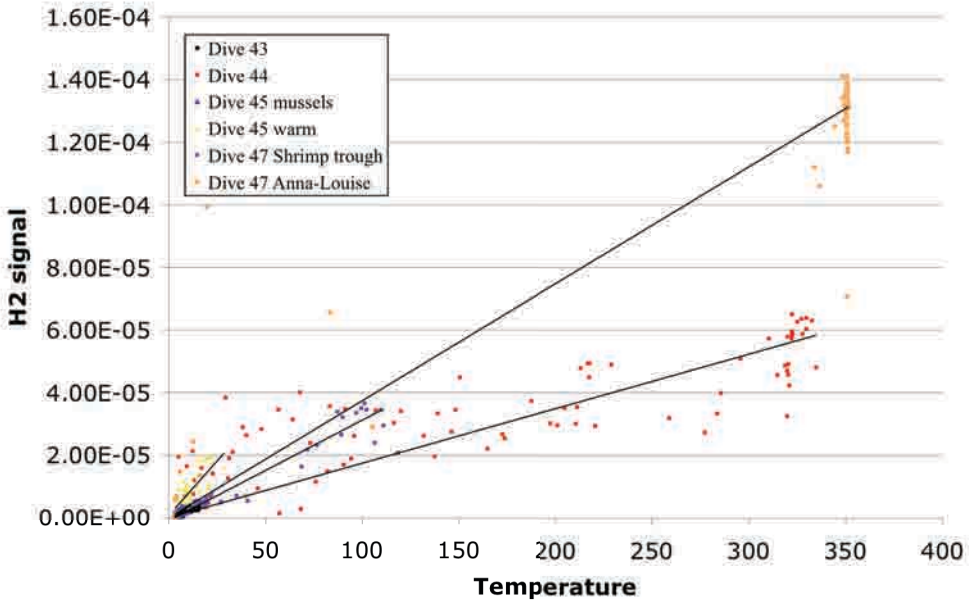

Fig. 5.19 Relationship of H_2 signal (partial pressure inside the instrument) with temperature in hot fluids emanating from Microsmoker (Dive 44), near mussels (Dives 43 and 45), in shimmering water near mussels (Dive 45 warm), in a among shrimp (Dive 47 shrimp trough), and in hot fluids of the Anna-Louise smoker (Dive 47 Anna-Louise).

Hot fluids

The ISMS was used on hot fluids during dives 44 (Microsmoker at the Irina II complex), 46 (Site B), and 47 (Anna-Louise smoker). The fluids emanating from the Microsmoker chimney showed very high concentrations of CO_2, H_2, and CH_4 (Fig. 5.20), correlated to increase in temperature and variations of pH values. The concentration of oxygen was negatively correlated to temperature data. Argon varied noticeably, also correlated to temperature readings.

A first recording near a group of shrimp (Fig. 5.20) on the chimney wall showed a slight decrease of oxygen and a strong increase of H_2 and CH_4 (these two latter similar to concentrations seen around mussels with shimmering water), along with CO_2, and the pH dropped to 7.5.

In the hot fluids, all these variations were more marked, with H_2 reaching a concentration of about 3-4 mM and CH_4 a concentration of about 400-600 µM. The pH value dropped down to 4.3 at the warmest time and constantly remained lower than 6 while in the hot fluids (figure 2, bottom).

At the Anna-Louise chimney (Dive 47), we sampled apparently pure fluids (very steady temperature), with H_2 concentrations in the order of 8-9 mM, and an in situ pH of 3.2 (the H_2/CH_4 ratio remained similar to other hot fluids).

Diffuse areas

Measurements were made near mussels, in a focused shimmering water source, and over a bacterial mat (marker 26). The signal was very small over the bacterial mat but clearly showed no H_2 anomaly, and some CH_4 and CO_2 anomaly. This difference could indicate consumption by mussels and/or subsurface biosphere.

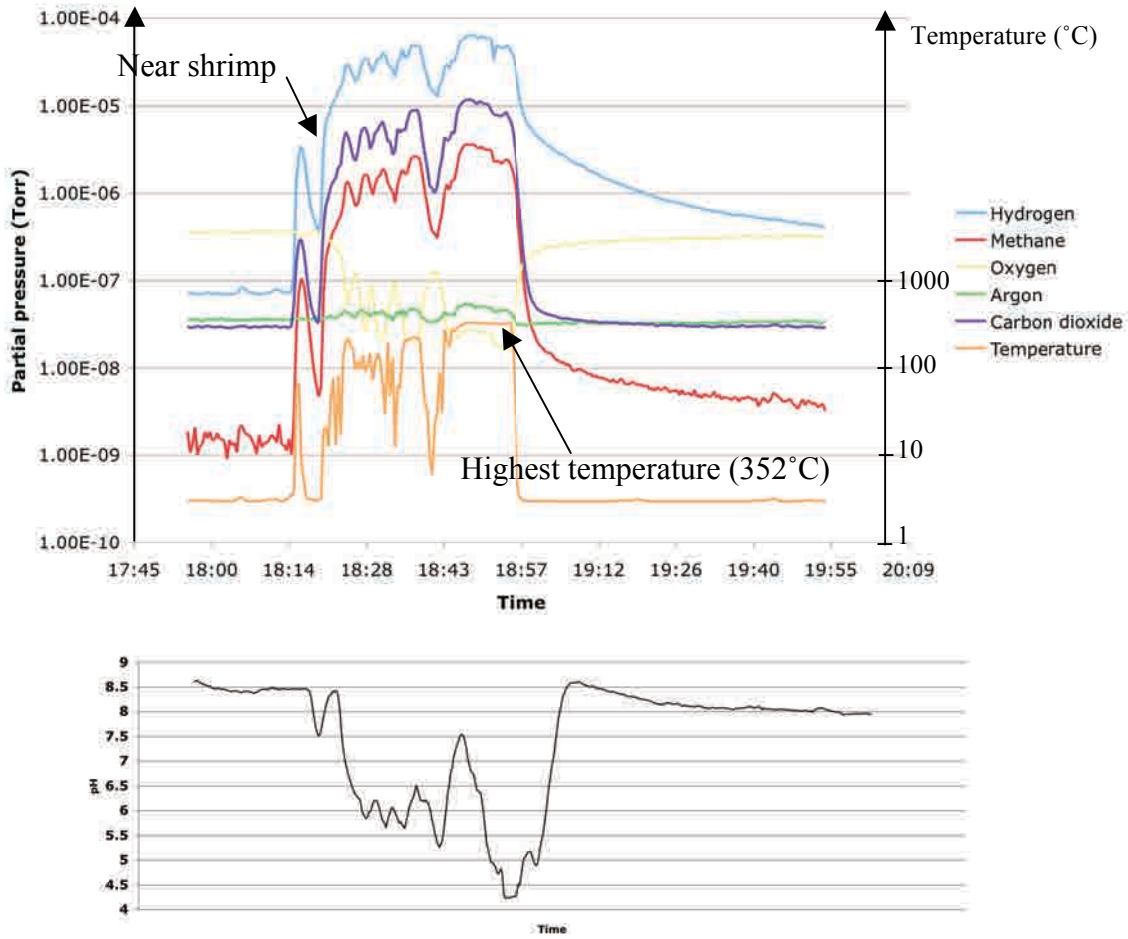

Fig 5.20 Recording of pH (lower panel) and various important gases (top panel) in the hot fluids emanating from Microsmoker. The values correspond to partial pressure of these gases (log scale). Time is in UTC.

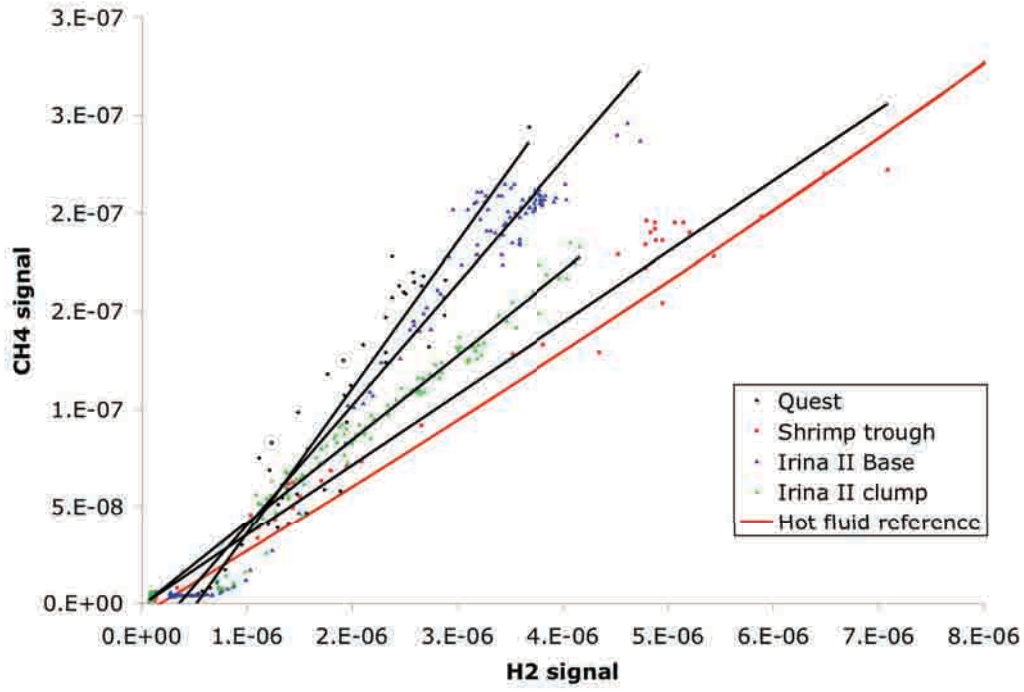

Fig. 5.21 CH_4/H_2 relationships for various mussel surveys, compared to a hot fluid reference (Microsmoker).

We measured the concentration of gases around 4 different mussel aggregations and compared these to the values obtained for different hot fluids (Fig. 5.21). Most water samples around mussels showed a depletion in H_2, with the noticeable exception of the Shrimp trough, a high-flow area with a small clear smoker at its base (110˚C at the hottest). These lower than expected H_2 values could indicate consumption by the mussels or a subsurface biosphere. Interestingly, the most depleted water was sampled around mussels that showed a high H_2 consumption rate (Quest mussel sample, see Symbiosis section below). Unfortunately, the limited number of dives did not allow us to do a clear-cut experiment and measure gases after the removal of all mussels from a point emission.

5.6 Microbiology

5.6.1 Microbial Ecology

(M. Perner, N. Rychlik)

5.6.1.1 Microbial Community Composition and its Functionality

The main objective of ourogy group during this cruise was to collect low-temperature, diffuse and hot hydrothermal fluids as well as a chimney piece from the Logatchev hydrothermal field to investigate:

- *the intra-field microbial variability and to continue the time-series studies*
- *the functioning of the microbial community, specifically focusing on microbial H_2- and H_2S-oxidation coupled to CO_2 fixation.*

However, due to bad weather and high waves we were restricted to five dives in total. During these dives, three hot hydrothermal fluid samples (Site B, Irina II and Anna Louise), a chimney piece (Site B) and two diffuse fluids were sampled from Irina II within the mussel patch in front of the Irina II mound. Additionally, we collected plume samples from the Logatchev I field by using the CTD. Therefore, during this cruise, we focused on investigating:

1. *vertical gradients within the Logatchev hydrothermal field I plume*
2. *the influence of distinct inorganic energy sources on microbially mediated autotrophic CO_2 fixation*
3. *small scale heterogeneity within the microbial community and short term variations of the microbial population at Irina II mussel bed*

For these investigations, material for DNA and *in situ* hybridization (Amann *et al.*, 1990; Pernthaler *et al.*, 2002) was collected and will be analyzed in the home laboratory (see Appendix sample Table 3.1). Additionally, multiple cultures selecting for hydrogen- and sulfide oxidizing autotrophs (see e.g. Nakagawa *et al.*, 2005) and heterotrophs were enriched.

1. Vertical microbial gradients within the Logatchev hydrothermal field I plume

Plume samples were collected from a depth of 3050 bar (264 CTD Niskin 1), from 2750 bar (264 CTD Niskin 7), 2550 bar (264 CTD Niskin 13) and at 2050 bar (264 CTD Niskin 15) (see Fig. 5.22).

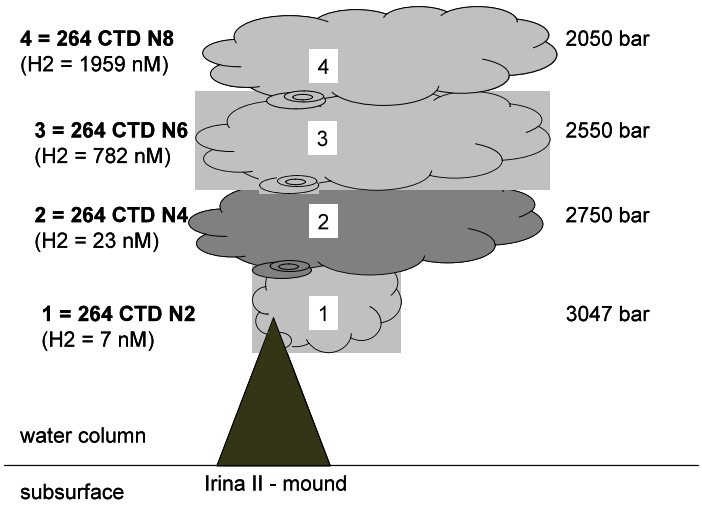

Fig. 5.22 Schematic overview of the plume samples collected during 264 CTD to investigate the vertical gradient of the plume. Samples for microbial analyses (DNA, in situ hybridization, and cultures) were collected according to the highest and lowest hydrogen concentrations detected in the corresponding samples by M. Warmuth and A. Heddaeus (see section 3.4.3). 1-4 indicate the different samples from the different Niskin bottles fired at the depths shown on the right.

2. The influence of distinct inorganic energy sources on microbially mediated autotrophic CO_2 fixation

We repeated experiments conducted on previous cruises (MSM 06-2 and 06-3) for investigating the influence of hydrogen and sulfide on microbially mediated autotrophic CO_2 fixation. For this, low-temperature, diffuse hydrothermal fluids from the mussel patch at Irina II (sample numbers 272 ROV 3. 4, 6) and from the plume (312 CTD 9) were sampled (Fig. 5.23).

Fig. 5.23 Sampling site in the mussel patch directly in front of the Irina II mound.

We supplemented the hydrothermal fluids/plume with either hydrogen (oxic, microaerophilic or anoxic conditions) or sulfide, added the inorganic radioactively labeled carbon, and incubated the liquids for 7-9 hours. Hydrogen uptake (M. Warmuth, University of Hamburg), sulfide concentrations (M. Peters, University of Münster), and incorporated amounts of inorganic carbon were determined. Some of this material was collected for microautoradiography and in situ hybridization. Also, parallels were performed for later 16S rRNA community analyses.

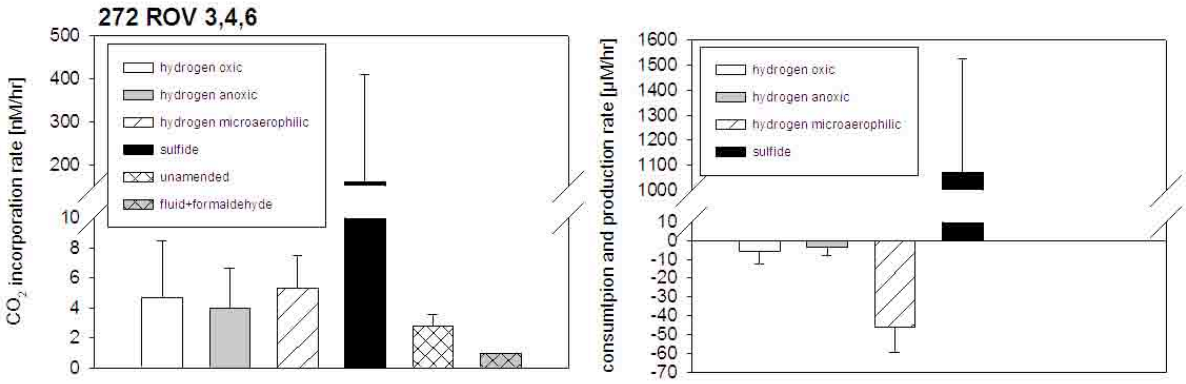

Fig. 5.24 CO_2 incorporation, consumption, and production rates measured for the fluids amended with hydrogen or sulfide. Hydrogen was measured by M. Warmuth (University of Hamburg) and sulfide concentrations were determined according to Cline (1969) by M. Peters (University of Münster).

Interestingly, the highest carbon incorporation rates were determined for the sulfide supplemented fluids (Fig. 5.24A). However, an increase of sulfide was observed in these incubations (Fig. 5.24B) and therefore the oxidation of a yet unknown energy source must be responsible for providing the energy for autotrophic CO_2 fixation. We also found that the largest amount of hydrogen was consumed under microaerophilic conditions with inorganic carbon being fixed (Fig. 5.24).

3. Small scale heterogeneity and short-term variations within the microbial community

For these analyses we collected diffuse fluids from the mussel bed at Irina II. From this site we already have a good dataset. Six KIPS bottles were collected from one site at the mussel field from Irina II inhabited by mussels forming a mound. These six bottles were treated as two samples (300 ROV 16-18 and 300 ROV 19-21) to investigate the short-term variability (Fig. 5.25A). A further two bottles (300 ROV 22-23) were taken from another site, approximately 40 cm away, to study the spatial heterogeneity (Fig. 5.25B). Material exists to analyze the microbial community by 16S rRNA and functional genes and in situ hybridization (see Appendix 3, Table 2).

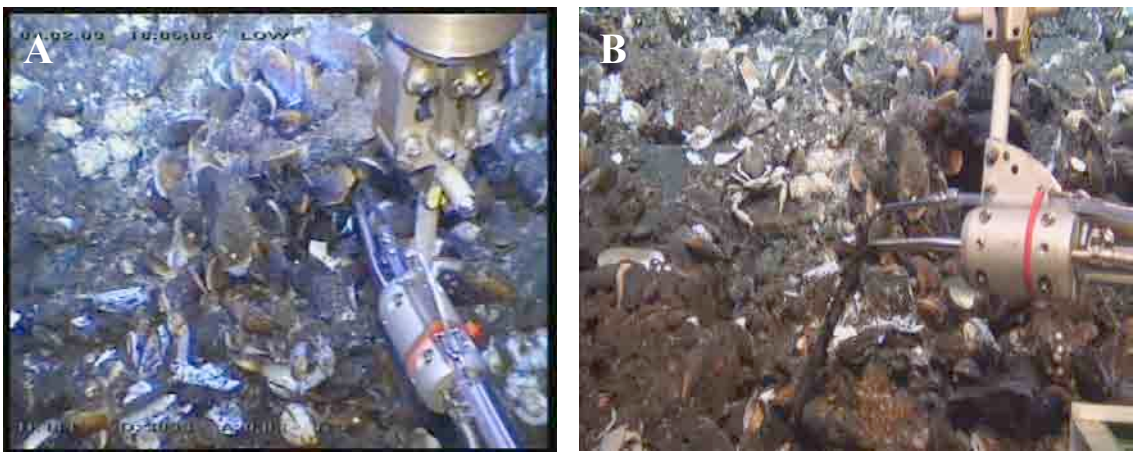

Fig. 5.25 Sampling of two spots in the mussel field at Irina II. Samples from spot 1 (A) were collected for investigating short-term variability and from spot 2 (B) for investigations of the spatial heterogeneity.

5.6.1.2 Metal-Complexation Experiments Using Culture

(V. Klevenz, M. Perner)

Microbial life at deep-sea hydrothermal vents is exposed to high concentrations of metals present in the venting fluids. Although some of them are biologically essential at low levels, these metals are toxic at high levels. However, toxicity of a metal for the microbes depends on its chemical speciation, as speciation determines the metal's bioavailability.

To study the influence of amino acids (AAs) as possible ligands for copper (Cu), with impact on the bioavailability of both (AAs constitute an energy source to microbes) and on the copper's toxicity we designed a culture experiment: Microbes derived from diffuse fluids of Irina 2 (from sample 300ROV 16-21) were cultured along Cu gradients (from 0 to 10 µM) and with three different concentrations of a mixture of 19 proteinogenic AAs (0, 100 nM and 1µM).

Shifts in the microbial communities will be monitored, and the concentration of labile Cu, i.e. not complexed by strong organic ligands, of total Cu and of Cu-ligands in the cultures, as well as of the vent sample the microbes are derived of, were measured by voltammetric methods (see section 3.4.4). Furthermore, the AA concentration in the fluid sample will be determined by the use of an HPLC-FD system. The total Cu concentration of the sample was determined after UV-digestion (2h) on board: [Cu] = 36 nM. The rest of the analyses will be carried out in the geochemistry lab at Jacobs University Bremen (voltammetric and HPLC analyses) and in the microbiology lab at University Hamburg (microbial communities).

5.6.2 Metagenomics: Diversity and Function of Chemosynthetic Microbial Communities in Hydrothermal Vent Sediments

(C. Huang)

The main goal of the Metagenomics group was to continue the investigation of microbial communities in different hydrothermally influenced sediments begun during the RV Meteor cruise M 64-2. Furthermore, from the preliminary research, sulphide oxidizers were known to be dominant in the areas we took our samples from. Fig. 5.16 shows the hypothesis we assumed based on the results of our experiments. Therefore, during the cruise, on board energy uptake experiments were also performed to see if H_2 and H_2S play a role as an electron donor.

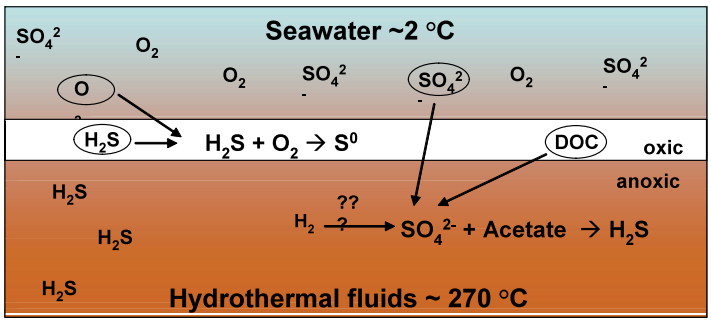

Fig. 5.26 Energy redox pairs hypothesis

Molecular/ microbial methods

Sediments were sampled using the Kiel6000 operated push cores. Immediately upon retrieval, the sediment cores were sectioned into slices of 1 or 2 cm. Sub-samples of each slice were frozen

at -80 °C for DNA extraction and diversity studies. 2 x 2 g of each slice were filled with 10ml RNA-later for RNA extraction. 5-10 g of sediments were frozen at -80 °C for metagenomic analyses. The rest of the slices were fixed with 50% ethanol in phosphate buffered saline (PBS) and 4% formaldehyde (FA/PBS) for 3-6 h, respectively, for cell count determination, and catalyzed reporter deposition fluorescence in situ hybridisation (CARDFISH).

For on board analyses of uptake rates of energy sources, 0,5 g of sediments were incubated with sulphide and hydrogen, and the decrease of these energy sources over time was measured in the headspace or fluid of the incubation vial. Vials with sterile filtered deep sea water (collected from CTD-rosette and filtered with 0.2 µm filters) or killed sediments or PFA 4% fixed sediments were used as controls.

Samples and preliminary results

Continuing investigations of sediment samples from M 64-2 and MSM 04-3 revealed a high microbial diversity. In particular, sediments with a characteristic white surface, Site F (Fig 5.27) showed strong differences in their bacterial and archaeal composition. This time we also took samples from a reference site, oceanic sediments, to better understand the difference between bacterial diversity and community.

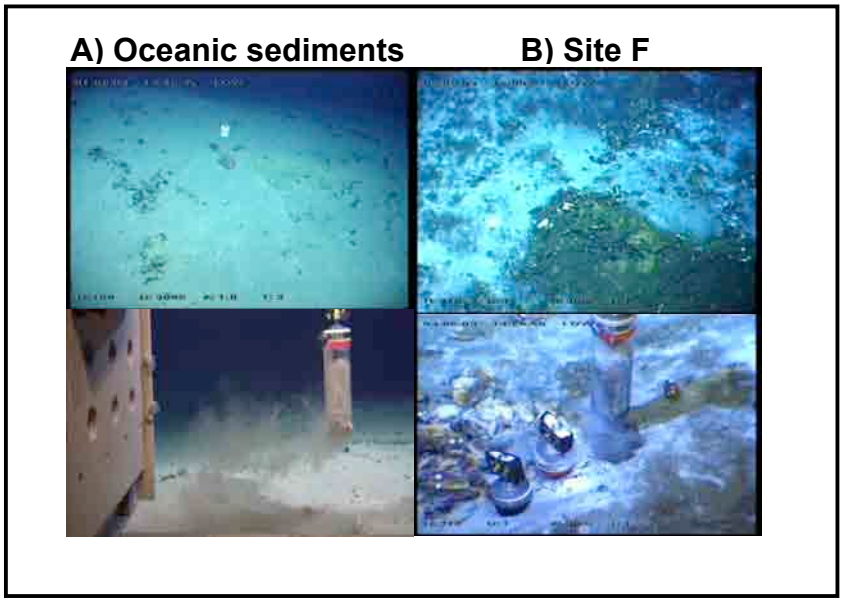

Fig. 5.27 A: Oceanic sediments: reference site. B: Site F, white mats

Uptake rates of different electron donors

After 30 minutes, 1 h, 3 h, and 6 h at 4°C incubation, sulphide concentration decreased and was clearly used as an energy source by the surface layer of sediments (Fig. 5.28). The mat on top of the surface showed a small decrease of sulphide in the beginning but after 1 h, it increased. In addition to sulphide, we also used hydrogen as an electron donor, but did not observe obvious uptake (Fig. 5.29). We assumed that the reactivity of the sediments is probably not as active as on the bottom. Perhaps next time we can try to increase the amount of sediments for this experiment. In summary, our first results indicate that sulphide can be used as an energy source by bacteria living in the surface layers of sediments. But for hydrogen, experimental conditions need to be optimized.

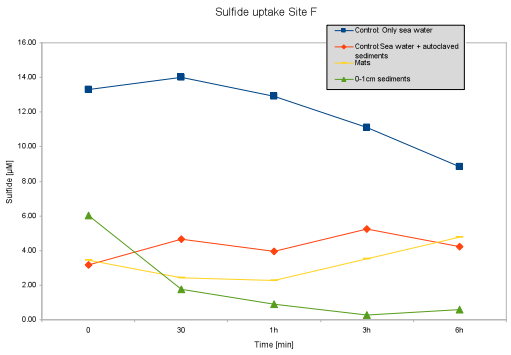

Fig. 5.28 Sulphide uptake experiments

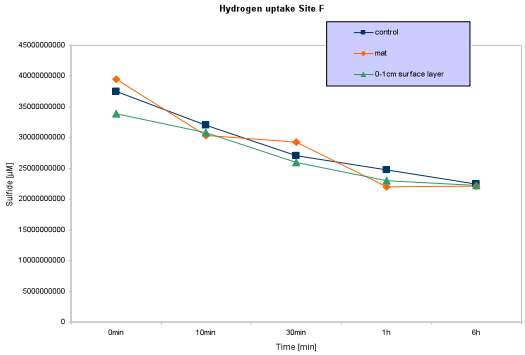

Fig. 5.29 Hydrogen uptake experiments

Diversity analyses and metagenomics

The push core samples obtained from the sites listed in Tab 5.3 will be used to investigate the microbial diversity of microbial communities in hydrothermally influenced sediments. The results will be compared with existing data to estimate the variability of the microbial communities in hydrothermally influenced sediments. We will test if diversities are homogeneous within cores and if single cores are representative for the microbial community of entire sites. A main focus will lie on investigations of the metabolic pathways of the dominant microorganisms in the selected sites. Fosmid libraries will be constructed and analysed for the inventory of functional genes indicating the metabolic capacities of the determined microorganisms. Apart from sediments, we also go into more detail investigations between white mats and surface layer of sediments. We expect more information on the diversity and possible ecological roles of these organisms by phylogenetic analyses on the basis of 16S rRNA including the screening of clone libraries and CARD-FISH experiments.

Tab. 5.3 Sampling locations of push cores

Site	location	sediment sample	position
Station	station number	station number	
Oceanic sediment (Reference site, Marker 21)	near OBT site	290 ROV-3	14°45.1942' N 44°58.7791' W
Site F (Marker 26)	white mat	300 ROV-2 300ROV-3 300 ROV-4	14°45.1356' N 44°58.7306' W

5.7 Hydrothermal Symbioses

(C. Borowski, D. Fink)

Our main goal for this cruise was to continue investigations on the transfer of energy from vent fluids to the mussels *Bathymodiolus puteoserpentis* which are dominant members of the faunal community at Logatchev. The fluids of the ultramafic hosted Logatchev vents are rich in methane and hydrogen but contain low concentrations of sulfide compared to other basaltic hosted vents on the Mid-Atlantic Ridge. Hydrogen is a very valuable energy resource for

chemoautotrophic organisms because its oxidation provides a higher energy yield per mol of oxidized electron donor than sulfide or methane. Free-living vent microbes able to use hydrogen as an energy source have been identified repeatedly, but its utilization by hydrothermal vent symbionts has never been shown.

Two types of symbionts coexist in the gills of *B. puteoserpentis*: chemolithoautotrophic bacteria that are considered to use reduced sulfur compounds such as sulfide as an energy source and fix CO_2 as a carbon source, and methanotrophic bacteria using methane both as an energy and carbon source. Our investigations during earlier cruises demonstrated that symbiont containing gill tissues of *B. puteoserpentis* mussels indeed consumed hydrogen and assimilated ^{14}C labeled inorganic carbon in incubation experiments with hydrogen as the only available electron donor. The use of hydrogen was evidenced during cruise MSM 04-3 for *B. puteoserpentis* specimens collected from the Quest vent, but similar experiments with animals from the Irina II mussel bed were lacking. Previous analyses of fluid compositions did not reveal significant differences between Quest and Irina II. However, Quest mussels appeared to be in a better physiological condition than Irina II mussels, as indicated for example by "fleshier" gills and a larger foot (Fig. 5.30). One goal for this cruise was therefore to continue earlier experiments and investigate if *Bathymodiolus* symbionts are similarly active in Irina II and Quest hosts and if Irina II symbionts also use hydrogen as an energy source. Ex situ experiments can not clarify which of the two symbionts or if both symbionts oxidize hydrogen. Another important goal was therefore to collect and prepare material for various molecular analyses with which hydrogen oxidizing pathways can be localized in *B. puteoserpentis* symbionts.

Fig. 5.30 *Bathymodiolus puteoserpentis* from Quest (left) and the Irina II mussel bed (right).

Mussels were collected by the ROV in close cooperation with sampling of diffuse fluids and in situ measurements of dissolved volatiles in various mussel microhabitats at the Quest and Irina II hydrothermal structures (see also sections 5.3 Gas Chemistry and 5.5 In situ Gas Measurements). In particular the real-time readings of biologically relevant dissolved volatiles such as O_2, H_2S, CH_4, H_2 and CO_2 by the in situ mass spectrometer (ISMS) together with simultaneous temperature measurements by the KIPS T-probe were used to characterize the geochemical milieus of the microhabitats and to select locations for mussel collections. The large time effort involved in dissecting and preparing mussels upon recovery for the ex situ experiments led us to concentrate on processing one mussel collection per dive to be able to always use only fresh animals. Five ROV dives provided five samples with animal material that served for experiments on board and for later analyses in the home laboratory (Tab 5.4).

Table 5.4 Mussel collection sites in the Logatchev hydrothermal vent field

Sample	Station number	Site	Coordinates
1	272 ROV 8	Irina II	14°45.1692' N, 44°58.7442' W
2	290 ROV 6	Irina II	14°45.1728' N, 44°58.7562' W
3	300 ROV 24	Irina II	14°46.1688' N, 44°58.7460' W
4	313 ROV 2	Quest	14°45.180' N, 44°58.829' W
5	315 ROV 8	Irina II	14°45.1782' N, 44°58.7460' W

Incubation experiments for measuring uptake rates of sulfide and hydrogen by gill tissues and use of these electron donors for primary production

We incubated symbiont-containing mussel tissue of *B. puteoserpentis* with different amounts of hydrogen and sulfide over time. Uptake rates of sulfide by mussel gill tissue showed differences between mussels from different sampling sites indicating that symbiont activity in Irina II mussels was higher than in Quest animals (Fig. 5.31). This result seemed to contrast our expectations of less symbiont activity in Irina II mussels, and several different explanations are possible. Although the gills of Irina II mussels appeared less well developed than those of Quest mussels, their symbionts may have been be more abundant or sulfide uptake metabolism was more active. Incubations with hydrogen as the only electron donor revealed that Irina II gill tissues also consume hydrogen (data not shown). These data need further calibration in the home laboratory, but in contrast to the sulfide assay, the raw data already indicated higher hydrogen consumption rates in Quest gill tissues than in Irina II gills. A possible role of variations in the composition of the diffuse fluids for different activity patterns can be estimated after thorough evaluation of the chemical fluid data and final calibration of the in ISMS measurements (which will be done in the P. Girguis laboratory in Harvard University). Molecular analyses of Irina II and Quest gill tissues in MPI-Bremen will reveal variations in patterns of symbiont abundances and also in symbiont activities.

To determine if consumption of sulfide and H_2 is used for symbiotic primary production, we incubated fresh gill material with radioactively labeled $NaH^{14}CO_2$ and Na_2S or H_2 as electron donors. The turnover of ^{14}C will be measured by scintillation counting in the home laboratory. Additional incubations with $NaH^{13}CO_2$ will be analyzed by nanoscale secondary ion mass spectrometry (nanoSIMS) which detects isotopic composition at a single cell level. NanoSIMS will visualize metabolically active cells, and we expect to be able to calculate their uptake rates and to determine nutrient fluxes.

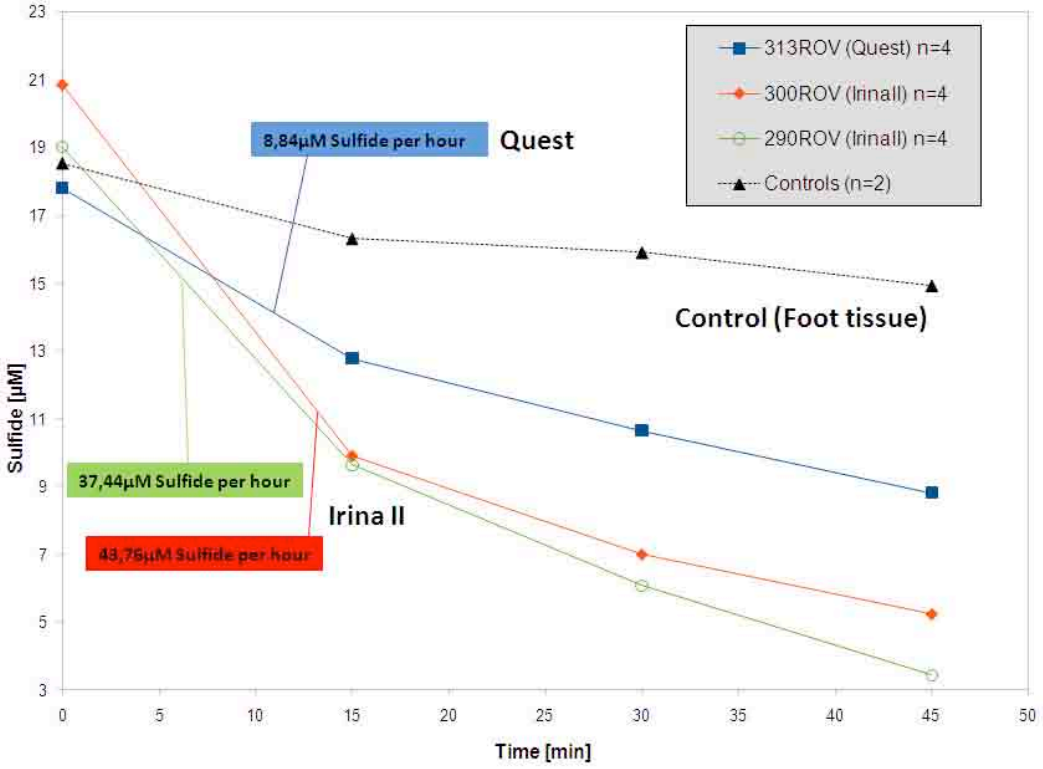

Fig. 5.31 Example of sulfide uptake by symbiont-containing gill tissues from *B. puteoserpentis* mussels from two vent sites measured as the decrease of dissolved sulfide in the incubation medium over time. Gill tissues pieces were incubated in 40 ml artificial seawater spiked with Na_2S at 20 mM end concentration. Initial decrease of sulfide after 15 min for Irina II mussels (4 mussels per dive, 2 dives) resulted in average sulfide uptake rates of around 40 µM h^{-1}. In contrast, Quest mussel gill tissues (4 mussels per dive, 1 dive) took up sulfide at a much slower initial rate of 8.84 µM h^{-1}. A decrease in sulfide concentration was also observed in incubations with symbiont-free foot tissues that served as controls. Differences between uptake rates of tissues with and without symbionts are attributed to uptake by symbiont activity.

Localization of the hydrogen oxidation pathway

Physiological ex situ experiments with *Bathymodiolus* gill tissues showed consumption and use of hydrogen, but did not reveal which symbiont is using the hydrogen. Information on the physiological potential of each symbiont can be gained by localizing genes encoding for key enzymes in physiological pathways provided the two co-occurring symbionts can be separated before DNA extraction. We aim at sequencing the genomes of the two *B. puteoserpentis* symbionts and another major goal for this cruise was to develop a method with which the two symbionts can be separated effectively from each other and host tissues. We variously modified a Histodenz density gradient centrifugation protocol that had been applied before for the separation of co-occurring symbionts in gutless oligochaetes and preserved the resulting fractions for later evaluations of the new protocols and preparations for genome sequencing in the home laboratories.

Search for free-living symbionts in the vent environment

A number of studies have suggested that *Bathymodiolus* mussels acquire their symbionts in each generation anew by uptake from the environment rather than by vertical transmission from parental generations to offspring. Consequently, free-living populations of the symbionts must exist in the mussel habitats, but such populations have never been detected in water samples or

by cultivations with diffuse fluids. Free-living symbionts of the giant tube worm *Riftia pachyptila* have been collected recently using colonization traps in a hydrothermal vent on the East Pacific Rise (Harmer *et al.*, 2008). This indicates that substrate colonizers may be attracted efficiently by deployed colonization surfaces even if their abundance in the water is very low. We developed colonization traps which allowed settlement of surface colonizing bacteria on microscopic slides and synthetic sponge material. The so called "Symcatchers" were deployed by the ROV for ten days in dense mussel aggregations at the basis of the Irina II sulfide structure (Fig. 5.32). After recovery, the slides and synthetic sponge were removed and fixed separately for fluorescence in situ hybridizations (slides) and DNA analyses from clone libraries (sponge) in the home laboratory.

Fig. 5.32 "Symcatcher" colonization traps for attracting free-living stages of mussel symbionts. Left: Before deployment. A PVC frame holds microscopic slides and synthetic sponge serving as colonization surfaces for free-living bacteria. Right: "Symcatcher" in the environment of a mussel bed at Irina II.

5.8 ROV Kiel 6000 and its Operation

(F. Abegg, M. Pieper, C. Hinz, H. Huusmann, I. Suck, W.Queisser, E. Labahn, P. Franke)

The ROV (remotely operated vehicle) Kiel 6000 is a 6000 m rated deep diving platform manufactured by Schilling Robotics LLC. As an electric work class ROV from the type QUEST, this is build no. seven, which is based at the Leibniz Institute for Marine Sciences IFM-GEOMAR in Kiel, Germany.

Mobilisation of Kiel 6000 started on Monday 10th of November after an emergency call due to technical problems of the QUEST 5 at the MARUM, Bremen. At that time, the ROV was still in Eckernfoerde/Germany for pilot training purposes. The ROV was transported back to the IFM-GEOMAR facility on December 1st where the final preparations started immediately. During December 8th and 9th, we received support from Stéphane Hourdez while integrating the ISMS (see section 5.5), which on one hand was well prepared with the help of Volker Ratmeyer (Marum, Bremen), who organised a junction box and cables, but in detail turned out to be a challenge due to incompatibility of the ISMS's and ROV's baud rates. Within two additional days, this problem was solved by integrating a baud-rate converter both into the ISMS and

behind the ROV output on the topside. Additionally, the KIPS (see 5.4) was integrated again with small modifications with the help of Dieter Garbe-Schoenberg.

The whole ROV equipment was shipped in the morning of December 19th via Bremerhaven to Las Palmas, where we received the containers on January 7th. In the evening of the 7th, we could set up the LARS, the containers were craned on deck on January 8th. From then on, the whole system was set up, which was finished with the harbour test on the 10th.

The UHD vehicle is equipped with 7 brushless thrusters, each of which with 210 kgf peak thrust. Power is supplied through the umbilical with up to 4160VAS/460 Hz. The data transfer between the vehicle and the topside control van is managed by the digital telemetry system (DTS™) which consists of two surface and four sub-sea nodes, each representing a 16-port module. Each port may be individually configured for serial, video or ethernet purposes.

The vehicle is linked to the topside control unit via a 19 mm diameter umbilical. No tether management system (TMS) is used. To unlink the vehicle from ship's movements, floats are attached to the umbilical. For more details please visit www.ifm-geomar/kiel6000.

Fig. 5.33 View of the ROV Kiel 6000 front with cameras, manipulators and tool sled

Tools permanently installed on the vehicle include a HDTV camera, two high-resolution colour zoom cameras and one digital still camera as well as four black and white observation cameras. Besides the video capabilities the two manipulator arms are the major tools used on this platform. One is a seven-function spatially controlled manipulator of the type ORION and the other one is five-function rate controlled manipulator, type RIGMASTER. Further tools include a DIGIQUARTZ depth sensor, a SIMRAD sonar system, a PNI TCM2-50 compass, a motion reference unit (MRU) containing a gyro compass, and an RDI doppler velocity log (DVL). A further tool used especially for navigation is the USBL-based IXSEA POSIDONIA™ system.

Additionally a SONARDYNE HOMER^{TM} system is available as a tool for navigation within a certain area of interest which has been marked with one or more HOMER beacons.

The tool sled in the lower-most part of the vehicle is especially dedicated to take up the scientific payload. Standardly there is a SBE 49 FastCAT CTD. Located on portside front of the tool sled is a sample tray which can be opened hydraulically. On starboard front there is a drawer likewise hydraulically driven, which can take up probes taken by the manipulator. Port aft and starboard aft are reserved for additional scientific payload which may differ from mission to mission.

The major scientific payload was the ISMS. As mentioned before, the integration and use of the ISMS was a challenge and realised the first time using a German research ROV. It was mounted together with a pump and a pH-sensor on a plate, which made it easier to take the system out of the ROV for maintenance purposes (see Fig. 5.34). The ISMS was located on the port aft space in the tool sled. The starboard side was occupied by the KIPS fluid sampling system. Additional tools for scientific samples during the cruise have been pushcores, mussel nets, the biobox, the anaerobic box, symbiont catchers and a Helium sampling tube. Details of these tools are given in the respective chapters.

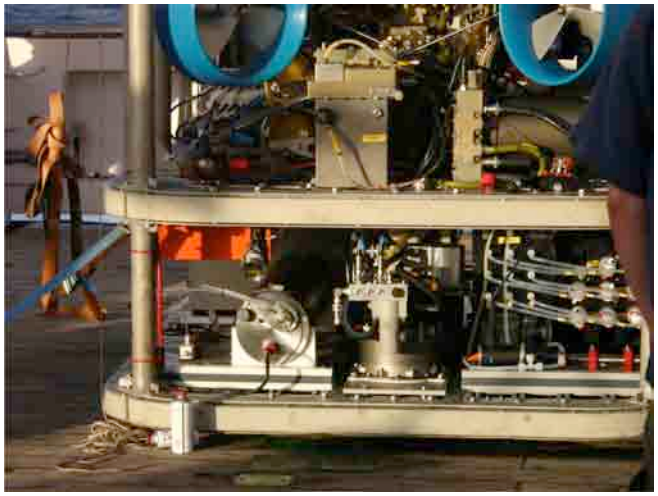

Fig. 5.34 Back side of the ROV with ISMS on the port side of the tool sled.

In total, there were 7 dives (Tab. 5.5) including one harbour test in Las Palmas and two test dives on a seamount, which was mapped during the transit into the working area.

Despite constantly adverse weather conditions with high winds (usually > 5 Bft) and high seas, we were able to carry out 5 successful scientific dives in the Logatchev hydrothermal vent field, summing up to more than 28 h bottom time. As during dive days wind and waves were only slightly lower than usual, recovery of the vehicle was a challenge. Conditions were severed by the recovery of heavy, long-term installed, gear, which additionally had to be carried on the porch. Still, we managed to recover the following gear: OBT, OBP, 2 SMonis, 5 temperature loggers.

The following measurements and sampling were routinely conducted during the dives: ISMS measurements, sampling of diffuse and hot fluids using KIPS, temperature measurements using KIPS, sampling of mussels using mussel nets. More singular/specific tasks included the sampling of sediments using push cores, the sampling of a piece of a smoker, sampling of wood (which was deposited on the seafloor 2 years ago) and sampling of hot fluids using the Helium

tube. A special bonus of the last dive was the videographing of the black smoker Bara-Dûr with the aim to get a data base for later 3-D reconstruction of the Black Smoker.

Navigation using POSIDONIA USBL showed to be almost perfectly precise, and start positions were generally found within seconds to few minutes.

Tab. 5.5 Summary of dives during HYDROMAR VII

Station # MSM 10/	Dive No	Date	Time Start (UTC)	At Bottom (UTC)	Off Bottom (UTC)	Time End (UTC)	ROV bottom time	% bottom time	Location
	39	10.01.2009							Harbour Test
234	40	13.01.2009	09:00			10:15			Test Dive Seamount
236	41	13.01.2009	15:26	16:32	17:24	18:26	0:56	31.0	Test Dive Seamount
272	42	25.01.2009	10:30	11:54	14:15	16:09	2:21	41.6	Logachev HVF
290	43	01.02.2009	12:05	13:36	19:54	21:18	6:18	68.3	Logachev HVF
300	44	04.02.2009	11:18	12:37	19:51	21:52	7:14	71.1	Logachev HVF
313	45	08.02.2009	14:22	15:33	20:00	21:35	4:33	65.5	Logachev HVF
315	46	09.02.2009	10:35	12:01	19:40	21:00	7:39	72.3	Logachev HVF
Total: 6 Dives							29:01h	58.3*	

*= without the test dive this number would be 63,8%

6 Ship's Meteorological Data

Station	Date 2009	Time [UTC]	W. strength [m/s]	Station	Date 2009	Time [UTC]	W. strength [m/s]
MSM10/233	13.01.	04:53	E 12	MSM10/275	26.01.	13:15	ENE 12
MSM10/234	13.01.	09:43	ENE 10	MSM10/276	26.01.	22:00	ENE 14
MSM10/235	13.01.	11:38	E 11	MSM10/277	27.01.	11:50	ENE 11
MSM10/236	13.01.	16:35	E 8	MSM10/278	27.01.	15:11	E 13
MSM10/237	13.01.	19:12	E 8	MSM10/279	27.01.	23:45	ENE 12
MSM10/238	17.01.	14:12	E 10	MSM10/280	28.01.	08:53	ENE 12
MSM10/239	17.01.	19:55	ENE 13	MSM10/281	28.01.	20:12	E 12
MSM10/240	18.01.	01:25	E 16	MSM10/282	29.01.	12:22	ENE 12
MSM10/241	18.01.	10:39	E 13	MSM10/283	29.01.	14:35	ENE 12
MSM10/242	18.01.	11:04	E 12	MSM10/284	30.01.	16:56	ENE 14
MSM10/243	18.01.	11:24	E 14	MSM10/285	31.01.	01:13	ENE 13
MSM10/244	18.01.	11:54	E 13	MSM10/286	31.01.	12:04	E 12
MSM10/245	18.01.	12:25	E 13	MSM10/287	31.01.	15:14	ENE 13
MSM10/246	18.01.	12:58	E 14	MSM10/288	31.01.	22:19	ENE 11
MSM10/247	18.01.	18:46	E 11	MSM10/289	01.02.	10:14	E 8
MSM10/248	20.01.	10:05	ENE 15	MSM10/290	01.02.	13:37	ENE 9
MSM10/249	20.01.	10:30	ENE 14	MSM10/291	01.02.	22:11	ENE 8
MSM10/250	20.01.	10:54	ENE 15	MSM10/292	02.02.	11:21	NE 14
MSM10/251	20.01.	11:25	ENE 15	MSM10/293	02.02.	14:15	ENE 11
MSM10/252	20.01.	11:56	ENE 15	MSM10/294	02.02.	16:14	ENE 11
MSM10/253	20.01.	12:25	ENE 15	MSM10/295	02.02.	19:50	ENE 14
MSM10/254	20.01.	14:22	ENE 14	MSM10/296	02.02.	21:17	ENE 13
MSM10/255	20.01.	15:55	NE 12	MSM10/297	03.02.	13:10	E 13
MSM10/256	20.01.	16:54	E 13	MSM10/298	03.02.	21:57	ENE 11
MSM10/257	20.01.	20:13	ENE 14	MSM10/299	03.02.	23:10	ENE 11
MSM10/258	21.01.	04:55	E 12	MSM10/300	04.02.	12:37	E 10
MSM10/259	21.01.	12:11	ENE 12	MSM10/301	05.02.	00:35	ENE 13
MSM10/260	21.01.	15:02	ENE 13	MSM10/302	05.02.	11:45	ENE 11
MSM10/261	21.01.	18:07	ENE 13	MSM10/303	05.02.	15:23	ENE 10
MSM10/262	21.01.	20:21	NE 10	MSM10/304	06.02.	00:04	ENE 13
MSM10/263	22.01.	12:57	ENE 10	MSM10/305	06.02.	11:53	E 13
MSM10/264	22.01.	17:46	ENE 13	MSM10/306	06.02.	15:57	E 12
MSM10/265	22.01.	21:27	E 12	MSM10/307	07.02.	00:45	E 12
MSM10/266	23.01.	11:54	E 13	MSM10/308	07.02.	11:47	E 10
MSM10/267	23.01.	16:15	ENE 10	MSM10/309	07.02.	15:25	ENE 11
MSM10/268	24.01.	00:51	E 14	MSM10/310	07.02.	20:37	ENE 9
MSM10/269	24.01.	12:15	E 14	MSM10/311	08.02.	03:32	ENE 10
MSM10/270	24.01.	15:48	ENE 12	MSM10/312	08.02.	12:29	ENE 11
MSM10/271	24.01.	22:47	ENE 9	MSM10/313	08.02.	15:35	E 10
MSM10/272	25.01.	11:52	E 12	MSM10/314	09.02.	02:00	ENE 9
MSM10/273	25.01.	18:16	E 12	MSM10/315	09.02.	12:01	E 6
MSM10/274	25.01.	20:53	ENE 13	MSM10/316	10.02.	20:23	ENE 8

7 Station List MSM 10-3

Station No./ Event label	Date 2009	Gear	Time [UTC]	Latitude [°N]	Longitude [°W]	WaterDepth [m]	Remarks/Recovery
MSM10/233	13.01.	EM120	04:53	26° 6.11' N	26° 15.02' W	5237.4	Start Profile
MSM10/234	13.01.	ROV	09:43	25° 45.00' N	26° 14.98' W	2652.3	ROV in water, technical issues, dive stopped
MSM10/235	13.01.	EM120	11:38	25° 55.25' N	26° 15.02' W	4396.7	Start Profile
MSM10/236	13.01.	ROV	16:35	25° 47.02' N	26° 14.25' W	1769.9	ROV at depth, start dive track
MSM10/237	13.01.	EM120	19:12	25° 41.54' N	26° 14.99' W	3886.8	Start Profile
MSM10/238	17.01.	CTD/RO	14:12	15° 5.74' N	44° 23.57' W	4864.9	At depth
MSM10/239	17.01.	MOR	18:45	14° 50.15' N	45° 1.03' W	3896.6	Start lowering Logatchev Mixing Mooring
MSM10/240	18.01.	EM120	01:25	14° 36.07' N	44° 44.97' W	3250.3	Start Profile
MSM10/241	18.01.	OBS	10:39	14° 46.25' N	45° 3.19' W	4175.9	OBS deployment, released at surface
MSM10/242	18.01.	OBS	11:04	14° 46.28' N	45° 0.61' W	3563.8	OBS deployment, released at surface
MSM10/243	18.01.	OBS	11:24	14° 46.47' N	44° 58.49' W	3043	OBS deployment, released at surface
MSM10/244	18.01.	OBS	11:54	14° 48.93' N	44° 55.93' W	2903.9	OBS deployment, released at surface
MSM10/245	18.01.	OBS	12:25	14° 48.95' N	45° 0.14' W	3614.8	OBS deployment, released at surface
MSM10/246	18.01.	OBS	12:58	14° 48.95' N	45° 4.33' W	3300.7	OBS deployment, released at surface
MSM10/247	18.01.	CTD/RO	18:46	15° 5.65' N	44° 23.50' W	4857.1	At depth
MSM10/248	20.01.	OBS	10:05	14° 43.63' N	45° 3.16' W	4172.4	OBS deployment, released at surface
MSM10/249	20.01.	OBS	10:30	14° 43.64' N	45° 1.11' W	4183.9	OBS deployment, released at surface
MSM10/250	20.01.	OBS	10:54	14° 43.63' N	44° 59.00' W	3319	OBS deployment, released at surface
MSM10/251	20.01.	OBS	11:25	14° 40.95' N	44° 57.37' W	3228.9	OBS deployment, released at surface
MSM10/252	20.01.	OBS	11:56	14° 40.96' N	45° 1.60' W	4016.5	OBS deployment, released at surface
MSM10/253	20.01.	OBS	12:25	14° 40.98' N	45° 5.76' W	3680.7	OBS deployment, released at surface
MSM10/254	20.01.	CTD/RO	14:22	14° 51.01' N	44° 58.81' W	3531.3	At depth
MSM10/255	20.01.	MAPR	15:55	14° 47.00' N	44° 58.82' W	3336.4	MAPR w/ dummy weight, stopped during descend at 31m depth
MSM10/256	20.01.	CTD/RO	16:54	14° 43.70' N	44° 58.82' W	3294.6	At depth
MSM10/257	20.01.	MAPR	20:13	14° 43.71' N	44° 58.82' W	3306.7	MAPR w/ dummy weight at depth, start towing
MSM10/258	21.01.	EM120	04:55	14° 49.68' N	44° 52.97' W	2791.6	Start Profile
MSM10/259	21.01.	CTD/RO	12:11	14° 49.98' N	45° 0.98' W	3958	At depth
MSM10/260	21.01.	CTD/RO	15:02	14° 50.99' N	44° 58.80' W	3480.1	At depth
MSM10/261	21.01.	CTD/RO	18:07	14° 48.00' N	44° 58.81' W	3384.9	At depth
MSM10/262	21.01.	EM120	20:21	14° 35.89' N	44° 56.95' W	3254.8	Start Profile
MSM10/263	22.01.	CTD/RO	12:57	14° 46.99' N	44° 58.84' W	3383.8	At depth
MSM10/264	22.01.	CTD/RO	17:46	14° 45.17' N	44° 58.75' W	3014.4	At depth
MSM10/265	22.01.	MAPR	21:27	14° 47.00' N	44° 58.82' W	3326.4	MAPR w/ dummy weight, at depth, start towing
MSM10/266	23.01.	CTD/RO	11:54	14° 47.50' N	44° 58.80' W	3337.3	At depth

MSM10/267	23.01.	MAPR	16:15	14° 46.66' N	44° 59.59' W	3616.5	MAPR w/ dummy weight, at depth, start towing
MSM10/268	24.01.	EM120	00:51	15° 0.22' N	45° 5.02' W	3046.6	Start Profile
MSM10/269	24.01.	CTD/RO	12:15	14° 47.01' N	44° 59.61' W	3666.2	At depth
MSM10/270	24.01.	CTD/TOWYO	15:48	14° 46.62' N	44° 59.59' W	3609.4	CTD/MAPR at depth, start towing
MSM10/271	24.01.	EM120	22:47	14° 36.03' N	45° 9.05' W	3385.5	Start Profile
MSM10/272	25.01.	ROV	11:52	14° 45.17' N	44° 58.71' W	3012.2	ROV at depth, start dive track
MSM10/273	25.01.	CTD/RO	18:16	14° 45.18' N	45° 1.08' W	3830.4	At depth
MSM10/274	25.01.	EM120	20:53	14° 44.78' N	45° 17.06' W	3201	Start Profile
MSM10/275	26.01.	CTD/TOWYO	13:15	14° 43.80' N	45° 1.08' W	4146.7	CTD/MAPR at depth, start towing
MSM10/276	26.01.	EM120	22:00	14° 49.48' N	44° 53.02' W	2749.7	Start Profile
MSM10/277	27.01.	CTD/RO	11:50	14° 43.21' N	44° 56.26' W	2721.2	At depth
MSM10/278	27.01.	CTD/TOWYO	15:11	14° 45.17' N	44° 58.70' W	3014.7	CTD/MAPR at depth, start towing
MSM10/279	27.01.	EM120	23:45	14° 55.49' N	45° 2.50' W	3710	Start Profile
MSM10/280	28.01.	CTD/YOYO	08:53	14° 45.18' N	45° 1.08' W	3811.2	An depth, start yo-yoing
MSM10/281	28.01.	EM120	20:12	14° 59.42' N	45° 10.01' W	3341.6	Start Profile
MSM10/282	29.01.	CTD/RO	12:22	14° 43.21' N	44° 56.26' W	2721.9	At depth
MSM10/283	29.01.	EM120	14:35	14° 51.60' N	44° 49.46' W	2664.2	Start Profile
MSM10/284	30.01.	CTD/YOYO	16:56	14° 45.18' N	45° 1.08' W	3799	An depth, start yo-yoing
MSM10/285	31.01.	EM120	01:13	14° 43.81' N	45° 1.18' W	4142.5	Start Profile
MSM10/286	31.01.	CTD/RO	12:04	14° 45.44' N	45° 0.43' W	3651.6	At depth
MSM10/287	31.01.	CTD/TOWYO	15:14	14° 43.62' N	45° 1.62' W	4134.2	CTD/MAPR at depth, start towing
MSM10/288	31.01.	EM120	22:19	14° 46.79' N	44° 58.71' W	3357.4	Start Profile
MSM10/289	01.02.	OBS	10:14	14° 43.58' N	44° 58.15' W	3021.1	OBS recovery, released
MSM10/290	01.02.	ROV	13:37	14° 45.19' N	44° 58.73' W	3016.7	ROV at depth, start dive track
MSM10/291	01.02.	EM120	22:11	14° 45.20' N	44° 57.95' W	2762	Start Profile
MSM10/292	02.02.	OBS	11:21	14° 43.49' N	45° 2.35' W	4093.2	OBS recovery, released
MSM10/293	02.02.	OBS	14:15	14° 46.86' N	45° 3.75' W	3966.1	OBS recovery, released
MSM10/294	02.02.	OBS	16:14	14° 45.89' N	44° 59.45' W	-	OBS recovery, released
MSM10/295	02.02.	CTD/RO	19:50	14° 43.21' N	44° 56.26' W	2711.2	At depth
MSM10/296	02.02.	EM120	21:17	14° 43.86' N	44° 56.17' W	2882	Start Profile
MSM10/297	03.02.	CTD/TOWYO	13:10	14° 43.38' N	45° 1.35' W	4153.9	CTD/MAPR at depth, start towing
MSM10/298	03.02.	CTD/RO	21:57	14° 46.00' N	44° 58.80' W	3211.9	At depth
MSM10/299	03.02.	EM120	23:10	14° 46.00' N	44° 58.25' W	3068.1	Start Profile
MSM10/300	04.02.	ROV	12:37	14° 45.15' N	44° 58.68' W	3003.3	ROV at depth, start dive track
MSM10/301	05.02.	EM120	00:35	14° 46.47' N	44° 41.69' W	3438.1	Start Profile
MSM10/302	05.02.	CTD/RO	11:45	14° 44.01' N	44° 58.82' W	3302.3	At depth
MSM10/303	05.02.	CTD/TOWYO	15:23	14° 43.52' N	45° 0.74' W	4078.5	CTD/MAPR at depth, start towing
MSM10/304	06.02.	EM120	00:04	15° 18.83' N	45° 21.23' W	3876.4	Start Profile
MSM10/305	06.02.	CTD/RO	11:53	14° 43.06' N	44° 58.82' W	3232.8	At depth
MSM10/306	06.02.	CTD/TOWYO	15:57	14° 43.39' N	45° 0.98' W	4161.9	CTD/MAPR at depth, start towing
MSM10/307	07.02.	EM120	00:45	15° 22.81' N	44° 36.58' W	4142.1	Start Profile
MSM10/308	07.02.	CTD/RO	11:47	14° 42.05' N	44° 58.87' W	3372.4	At depth
MSM10/309	07.02.	CTD/TOWYO	15:25	14° 44.10' N	45° 3.35' W	4248.6	CTD/MAPR at depth, start towing
MSM10/310	07.02.	CTD/TOWYO	20:37	14° 44.29' N	45° 3.10' W	4195.1	CTD/MAPR at depth, start towing
MSM10/311	08.02.	EM120	03:32	14° 28.19' N	44° 37.08' W	3353.5	Start Profile

MSM10/312	08.02.	CTD/RO	12:29	14° 45.17' N	44° 58.76' W	3017.6	At depth
MSM10/313	08.02.	ROV	15:35	14° 45.19' N	44° 58.80' W	3047.3	ROV at depth, start dive track
MSM10/314	09.02.	EM120	02:00	14° 28.28' N	45° 15.09' W	2546.4	Start Profile
MSM10/315	09.02.	ROV	12:01	14° 45.18' N	44° 58.69' W	3007.9	ROV at depth, start dive track
MSM10/316	10.02.	EM120	20:23	14° 57.99' N	50° 3.54' W	3462.3	Start Profile

8 Data and Sample Storage and Availability

The PIs of the scientific disciplines on board or their group leaders are responsible for data processing. These are: Bathymetric mapping and OBS data: I. Grevemeyer (IfM-Geomar); CTD data: M. Visbek, J. Fischer (IfM-Geomer), MAPR: C. Borowski (MPI-Bremen); Microbiology: M. Perner (Univ. Hamburg); Metagenomics: R. Amann (MPI-Bremen); Symbioses: N. Dubilier (MPI-Bremen); Fluid geochemistry: D. Garbe-Schönberg (Univ. Kiel), A. Koschinsky (JUB), H. Strauß (Univ. Münster); Dissolved gases: M. Warmut/R. Seifert (Univ. Hamburg); In situ mass spectrometry; P. Girguis (Harvard Univ.). Long term storage of processed and quality checked data will be in the Pangaea database and accepted genetic databases such as EMBL or Genbank.

9 Acknowledgements

R/V MARIA S. MERIAN cruise MSM 10-3 was an interdisciplinary research activity on the geology, chemistry, and biology of hydrothermal vents at the Logatchev hydrothermal vent field at 15°N on the Mid-Atlantic Ridge within the DFG Priority Program SPP1144. The cruise was planned and coordinated by MPI-Bremen, with the help of the involved institutions. The cruise was financed in Germany by the German Research Foundation (DFG). The shipping operator (Briese Schiffahrt GmbH & Co, Leer) provided technical support for the vessel to accommodate the large variety of technical challenges required for the complex sea-going operations. We would like to especially acknowledge the Master of the vessel, Friedhelm von Staa, his Chief mate Ralf Schmidt and their crew for their continued contribution to a successful research program and a pleasant and professional atmosphere aboard R/V MARIA S. MERIAN.

10 References

Amann, R.I., Binder, B.J., Olson, R.J., Chisholm, S.W., Devereux, R., Stahl, D.A. 1990. Combination of 16S rRNA-targeted oligonucleotide probes with flow cytometry for analyzing mixed microbial populations. Applied and Environmental Microbiology 56 (6), 1919-1925.

Charlou, J.L., Donval, J.P., Fouquet, Y., Jean-Baptiste, P., Holm, N., 2002. Geochemistry of high H-2 and CH4 vent fluids issuing from ultramafic rocks at the Rainbow hydrothermal field (36 degrees 14 ' N, MAR). Chemical Geology 191 (4), 345-359.

Cline, J., 1969. Spectrophotometric determination of hydrogen sulfide in natural waters. Limnology and Oceanography 14, 454-458.

Douville, E., Charlou, J.L., Oelkers, E.H., Bienvenu, P., Colon, C.F.J., Donval, J.P., Fouquet, Y., Prieur, D., Appriou, P., 2002. The rainbow vent fluids (36 degrees 14 ' N, MAR): the influence of ultramafic rocks and phase separation on trace metal content in Mid-Atlantic Ridge hydrothermal fluids. Chemical Geology 184 (1-2), 37-48.

Ferron, B., Mercier, H., Speer, K., Gargett, A., Polzin, K., 1998. Mixing in the Romanche Fracture Zone. Journal of Physical Oceanography 28 (10), 1929-1945.

Fouquet, Y., Cherkashov, G., Charlou, J.L., Ondréas, H., Birot, D., Cannat, M., Bortnikov, N., Silantyev, S., Sudarikov, S., Cambon-Bonavita, M.A., Desbruyères, D., Fabri, M.C.,

Querellou, J., Hourdez, S., Gebruk, A., Sokolova, T., Hoisé, E., Mercier, E., Kohn, C., Donval, J.P., Etoubleau, J., Normand, A., Stephan, M., Briand, P., Crozon, J., Fernagu, P., Buffier, E., 2008. Serpentine cruise - ultramafic hosted hydrothermal deposits on the Mid-Atlantic Ridge: First submersible studies on Ashadze 1 and 2, Logatchev 2 and Krasnov vent fields. InterRidge News 17, 15-17.

Harmer, T.L., Rotjan, R.D., Nussbaumer, A.D., Bright, M., Ng, A.W., DeChaine, E.G., Cavanaugh, C.M., 2008. Free-living tube worm endosymbionts found at deep-sea vents. Applied and Environmental Microbiology 74 (12), 3895-3898.

Keir, R.S., Schmale, O., Seifert, R., Sültenfuss, J., 2009. Isotope fractionation and mixing in methane plumes from the Logatchev hydrothermal field. Geochemistry Geophysics Geosystems 10.

Nakagawa, S., Takai, K., Inagaki, F., Hirayama, H., Nunoura, T., Horikoshi, K., Sako, Y., 2005. Distribution, phylogenetic diversity and physiological characteristics of epsilon-*Proteobacteria* in a deep-sea hydrothermal field. Environmental Microbiology 7 (10), 1619-1632.

Pernthaler, A., Pernthaler, J., Amann, R., 2002. Fluorescence in situ hybridization and catalyzed reporter deposition for the identification of marine bacteria. Applied and Environmental Microbiology 68 (6), 3094-3101.

Schmidt, K., Koschinsky, A., Garbe-Schönberg, D., de Carvalho, L.M., Seifert, R., 2007. Geochemistry of hydrothermal fluids from the ultramafic-hosted Logatchev hydrothermal field, 15 degrees N on the Mid-Atlantic Ridge: Temporal and spatial investigation. Chemical Geology 242 (1-2), 1-21.

Von Damm, K.L., Edmond, J.M., Grant, B., Measures, C.I., Walden, B., Weiss, R.F., 1985. Chemistry of submarine hydrothermal solutions at 21°N, East Pacific Rise. Geochimica Et Cosmochimica Acta 49, 2197–2220.